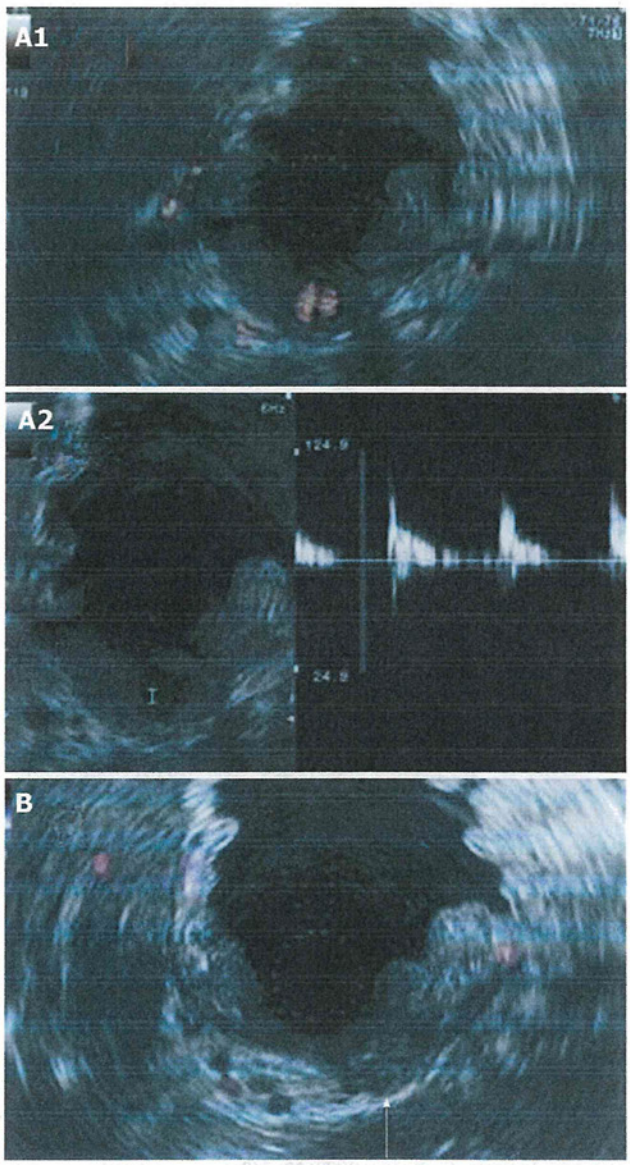

Figure 4 Endoscopic ultrasonography findings. A1: Endoscopic ultrasonography showed an anechoic region whose entire periphery was hypoechoic beneath the gastric mucosa. Power Doppler showed blood flow in the anechoic region. Upper gastrointestinal endoscopy showed a 2 cm, submucosal tumor-like protrusion with a red, eroded upper region located in the lesser curvature of middle of the body of the stomach (arrow); A2: Pulsed wave Doppler showed pulsatile blood flow in the anechoic region. This finding led to the diagnosis of an aneurysm; B: The cessation of blood flow to the pseudoaneurysm was confirmed with endoscopic ultrasonography which was performed 1 wk after treatment (arrow).

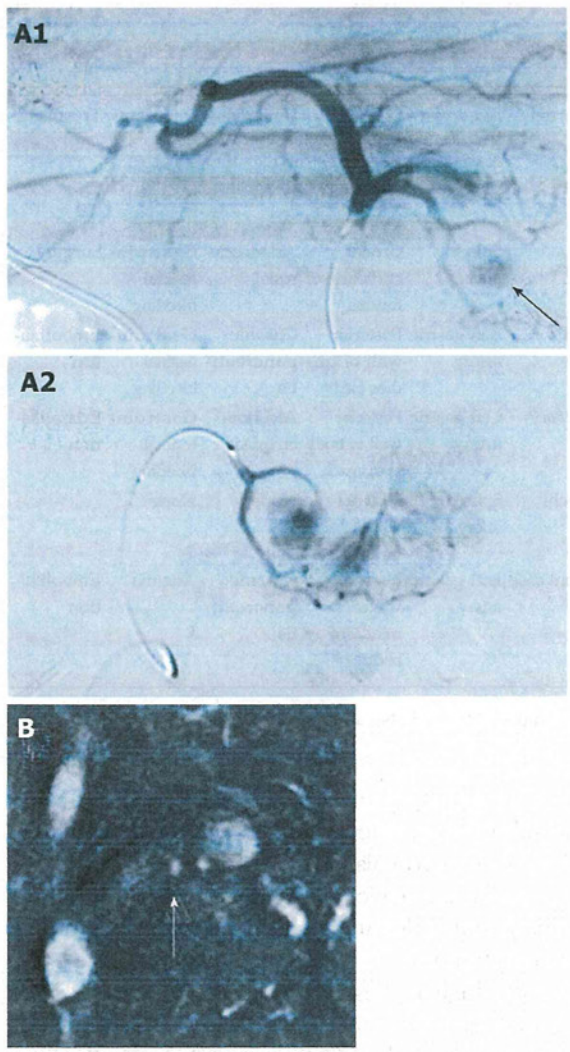

Figure 5 Angiography findings. A1: The pseudoaneurysm of the left gastric artery was diagnosed on angiography (arrow). The left hepatic artery diverged from the left gastric artery; A2: The microcatheter was advanced in the region of the pseudoaneurysm, and the pseudoaneurysm was embolized with histoacryl and lipiodol; B: A small pseudoaneurysm was observed in the splenic artery (arrow), and the splenic artery was embolized by coils.

mission revealed a communication between the tail duct and the pseudocyst. It is thought that the splenic pseudoaneurysm was bleeding into the pseudocyst because the splenic artery was adjacent to the pseudocyst on MDCT. No bleeding from Vater's papilla was observed when carrying out ERCP, but it was presumed that hemosuccus was the cause of this bleeding as the patient had black stool in the week preceding admission and was markedly anemic upon admission. The resulting progress of anemia triggered the discovery of a pseudoaneurysm in the left gastric artery which was on the verge of rupturing.

Although a pseudoaneurysm complicating chronic pancreatitis occurs relatively infrequently and affects only 6% to 9% of patients[1], 40% to 60% of ruptured pseudoaneurysms result in a fatal outcome[2]. Pseudoaneurysms are primarily attributed to the digestion and lysis of the arterial wall near the pancreas by errant activated pancreatic enzymes[3]. The splenic artery is the most commonly affected site. Pseudoaneurysms also frequently form in the gastroduodenal, pancreaticoduodenal, and hepatic arteries, but rarely in the left gastric artery[4,5]. Aneurysms of the left gastric artery mimicking a gastric submucosal tumor are also extremely rare[2,4].

The MDCT examination performed on admission may have missed the aneurysm because the lesion was small or because collateral circulation attributable to pancreatitis-induced pancreatic arteriovenous occlusion resulted in the imaging of many winding blood vessels which, in turn, complicated the identification and diagnosis of the aneurysm. EUS, which can show the gastric

Table 1 Cases of pseudoaneurysm diagnosed on endoscopic ultrasonography

Reported by	Aneurysm site	SMT-like lesion site	Underlying disease	Symptoms	Treatment
Mosler *et al*[7]	Splenic artery	Posterior wall of cardiac part	None	Anemia	
Chaya *et al*[8]	Splenic artery	Greater curvature of fundus	Arteriosclerosis	Gastrointestinal bleeding	Surgery
Falodia *et al*[2]	Left gastric artery	Posterior wall of cardiac part	Chronic pancreatitis	Gastrointestinal bleeding	Embolization
Jani *et al*[9]	Left gastric artery	Posterior wall of body of stomach	Alcoholic cirrhosis	Gastrointestinal bleeding	Embolization
Higuchi *et al*[10]	Splenic artery × 4	Posterior wall of fundus	None	None	-
Present case 2011	Left gastric artery	Lesser curvature of middle of body	Chronic pancreatitis	Anemia	Embolization

SMT: Submucosal tumor; -: No description.

wall in fine detail, is an excellent tool for diagnosing gastric submucosal lesions[6]. The added Doppler functionality of the particular EUS device used in the present case made the device better suited than MDCT for diagnosing and following small aneurysms resembling submucosal tumors.

Recently, higher rates of detection have been related to the increased frequency of imaging studies such as EUS[5]. A search of the literature revealed only this case and 8 other cases of submucosal tumor-like protrusions diagnosed as pseudoaneurysms on EUS[2,7-10]. The responsible vessel was the splenic artery in 6 cases and the left gastric artery in 3. The submucosal tumor-like lesion was often located in the fundus or cardiac area (7 of 9) and posterior wall (7 of 9). Two of the patients had chronic pancreatitis, one had alcoholic cirrhosis, one had arteriosclerosis, and five had no underlying disease. The lesions were coincidentally discovered during upper gastrointestinal endoscopic screening in four of these patients. Three of the patients had gastrointestinal bleeding that was treatable with either embolization or surgery (Table 1).

The danger of re-bleeding after embolization increases if pancreatitis continues even following treatment, but we believe that we were able to successfully control bleeding by avoiding stent implantation in the pancreatic duct and by avoiding bleeding. A pseudoaneurysm should be suspected when a gastric submucosal tumor-like protrusion is seen in a patient with chronic pancreatitis. We recommend that EUS be carried out, and if a pseudoaneurysm is diagnosed, then interventional radiology should be performed as soon as possible. In addition, the successful control of pancreatitis was believed to be the key to successful bleeding control.

REFERENCES

1 **Stabile BE**, Wilson SE, Debas HT. Reduced mortality from bleeding pseudocysts and pseudoaneurysms caused by pancreatitis. *Arch Surg* 1983; **118**: 45-51

2 **Falodia S**, Garg PK, Bhatia V, Ramachandran V, Dash NR, Srivastava DN. EUS diagnosis of a left gastric artery pseudoaneurysm and aneurysmogastric fistula seen with a massive GI hemorrhage (with video). *Gastrointest Endosc* 2008; **68**: 389-391

3 **Lee MJ**, Saini S, Geller SC, Warshaw AL, Mueller PR. Pancreatitis with pseudoaneurysm formation: a pitfall for the interventional radiologist. *AJR Am J Roentgenol* 1991; **156**: 97-98

4 **Marilley M**, Prabhukhot R, Astin M, Chiang K. Left gastric pseudoaneurysmal hemorrhage: a rare endoscopic detection. *Gastrointest Endosc* 2010; **71**: 871-873

5 **Elazary R**, Abu-Gazala M, Schlager A, Shussman N, Rivkind AI, Bloom AI. Therapeutic angiography for giant bleeding gastro-duodenal artery pseudoaneurysm. *World J Gastroenterol* 2010; **16**: 1670-1672

6 **Papanikolaou IS**, Triantafyllou K, Kourikou A, Rösch T. Endoscopic ultrasonography for gastric submucosal lesions. *World J Gastrointest Endosc* 2011; **3**: 86-94

7 **Mosler P**, Mergener K, Düber C, Bierbach H, Galle PR. Large splenic artery aneurysm mimicking a gastric submucosal tumor. *Endoscopy* 2000; **32**: S43

8 **Chaya CT**, Luthra G, Ernst R, Bhutani MS. A subepithelial mass determined by EUS to be a splenic artery aneurysm. *Gastrointest Endosc* 2007; **65**: 153-14; discussion 154

9 **Jani ND**, McGrath KM. Left gastric artery aneurysm. *Gastrointest Endosc* 2008; **67**: 154-15; commentary 155

10 **Higuchi N**, Akahoshi K, Honda K, Matsui N, Kubokawa M, Motomura Y, Nakamura K, Takayanagi R. Diagnosis of a small splenic artery aneurysm mimicking a gastric submucosal tumor on endoscopic ultrasound. *Endoscopy* 2010; **42** Suppl 2: E107-E108

S- Editor Yang XC **L- Editor** Webster JR **E- Editor** Yang XC

Identification of a DNA methylation marker that detects the presence of lymph node metastases of gastric cancers

YASUYUKI SHIGEMATSU[1], TOHRU NIWA[1], SATOSHI YAMASHITA[1], HIROKAZU TANIGUCHI[2], RYOJI KUSHIMA[2], HITOSHI KATAI[3], SEIJI ITO[4], TETSUYA TSUKAMOTO[5], MASAO ICHINOSE[6] and TOSHIKAZU USHIJIMA[1]

[1]Division of Epigenomics, National Cancer Center Research Institute, Chuo-ku, Tokyo 104-0045; Divisions of [2]Pathology and Clinical Laboratory and [3]Gastric Surgery, National Cancer Center Hospital, Chuo-ku, Tokyo 104-0045; [4]Department of Gastroenterology, Aichi Cancer Center Hospital, Chikusa-ku, Aichi 464-8681; [5]Department of Diagnostic Pathology, School of Medicine Fujita Health University, Kutsukake-cho, Toyoake, Aichi 470-1192; [6]Second Department of Internal Medicine, Wakayama Medical University, Kimiidera, Wakayama 641-8509, Japan

Received December 8, 2011; Accepted May 3, 2012

DOI: 10.3892/ol.2012.708

Abstract. The accurate detection of the presence of lymph node metastases (LNM) of gastric cancers (GCs) is useful for the implementation of necessary and sufficient treatment, but current methods of detection are unsatisfactory. In the present study, we focused on DNA methylation markers since they have several advantages, including biological and chemical stability and informativeness even in the presence of contaminating cells. Using three metastatic lymph nodes and three primary GCs without LNM, methylation bead array analyses were performed, which enabled the interrogation of 485,577 CpG sites. A total of 31 CpG sites that were hypermethylated in the metastatic lymph nodes, compared with the GCs without LNM, were isolated. Using primary GCs with and without LNM (28 GCs with LNM and 10 without), their methylation levels were measured using quantitative PCR following treatment with sodium bisulfite or a methylation-sensitive restriction enzyme. Of the genomic regions around the 31 CpG sites, 10 regions demonstrated higher methylation levels in the GCs with LNM compared with the GCs without LNM ($P<0.05$). Finally, the hypermethylation of the 10 regions was validated using another set of samples (129 GCs with LNM and 20 without). Hypermethylation of the region around the cg06436185 CpG site predicted the presence of LNM at a sensitivity of 43% and specificity of 85%. Additionally, the hypermethylation of the region was associated with a poor survival rate among GC patients with LNM. The results of the present study indicated that the methylation status of the region was a promising candidate marker to detect the presence of LNM of GCs and may reflect the malignant potential of GCs.

Correspondence to: Dr Toshikazu Ushijima, Division of Epigenomics, National Cancer Center Research Institute, 1-1 Tsukiji 5-chome, Chuo-ku, Tokyo 104-0045, Japan
E-mail: tushijim@ncc.go.jp

Key words: DNA methylation, gastric cancer, lymph node, metastasis

Introduction

Gastric cancer (GC) is one of the most prevalent malignancies worldwide and remains a leading cause of cancer-related mortality (1,2). Since the presence of lymph node metastases (LNM) is associated with a significantly poorer prognosis of GC patients (3-5), radical resection with free-margin gastrectomy and extended lymphadenectomy are performed for patients with advanced GC to eradicate LNM (6). Such an aggressive resection of the lymph nodes is associated with higher patient morbidity and/or mortality rates (7-9). Alternatively, the absence of LNM allows for minimally invasive surgery, which provides an improved quality of life following treatment. Therefore, the accurate detection of LNM is useful for the implementation of necessary and sufficient treatment.

To detect the presence of LNM, much effort has been made in the fields of imaging and molecular markers. Imaging modalities, including computed tomography (CT), endoscopic ultrasonography (EUS) and ^{18}F-fluorodeoxyglucose positron emission tomography (FDG-PET) are used in clinical practice. However, the sensitivities of these modalities are 77.2, 82.8 and 71%, respectively, and the specificities are 78.3, 74.2 and 74%, respectively (10-13). Moreover, these imaging modalities are almost powerless to detect micrometastases (14,15). With regard to molecular markers, analyses that targeted specific RNA and protein expression have been made. Although a number of these markers were associated with the presence of LNM of GCs (16-19), their utility has not been confirmed by independent studies. Therefore, genome-wide or comprehensive analysis of molecular markers for LNM of GCs is required and validation of the utility of the markers is essential for clinical application.

As a molecular marker, DNA methylation is advantageous, as its status is stable even if a cell is placed in different environments (biologically stable) and DNA is chemically stable, even in clinical materials. In addition, DNA methylation profiles are not disturbed by the presence of a small population of contaminating cells. As a strategy, we used metastatic lymph nodes and primary GCs without LNM for genome-wide analysis as cells with the abililty of LNM may constitute only a small population of the cells in primary GCs with LNM. Differences in methylation levels may be extremely small and may not be detected by the analysis between primary GCs with and without LNM. Alternatively, in metastatic lymph nodes, cancer cells are expected to possess the aberrant DNA methylation following clonal selection. Moreover, the methylation levels of appropriate marker CpG sites in the metastatic lymph nodes are expected to be relatively high compared with those in primary GCs with LNM.

In the present study, we aimed to identify CpG sites with a methylation status associated with the presence of LNM of GCs via a genome-wide methylation analysis using metastatic lymph nodes and primary GCs without LNM and to validate the isolated candidate markers.

Materials and methods

Patients, tissue samples and DNA extraction. A total of 187 GC surgical samples were obtained from patients who underwent gastrectomy with extended lymph node dissection (D2) at the National Cancer Center Hospital (Tokyo, Japan) and Aichi Cancer Center Hospital (Aichi, Japan) between 1994 and 2011 with informed consent. A total of three metastatic lymph nodes were obtained from 3 of the 187 patients. No patients had undergone prior chemotherapy or radiotherapy. Prognostic information of 55 GC patients with LNM was available and the mean follow-up period after surgery was 3,024 days. Disease grades were classified according to the 6th edition of the TNM classification by the UICC. Samples were stored at -80˚C and a high molecular weight DNA was extracted using the phenol/chloroform method. The 187 samples were divided into screening (28 GCs with LNM and 10 without) and validation (129 GCs with LNM and 20 without) sets in advance, between which no significant differences in clinicopathlogical data were observed (Table I). This study was conducted with the approval of the Aichi Cancer Center and National Cancer Center.

Genome-wide methylation analysis. Genome-wide screening of differentially methylated CpG sites was performed using an Infinium HumanMethylation450 BeadChip array, which covers 485,577 CpG sites (Illumina, San Diego, CA, USA) (20). Genomic DNA (1 μg) was treated with sodium bisulfite using a Zymo EZ DNA Methylation kit (Zymo Research, Irvine, CA, USA) and the bisulfite-modified DNA was amplified prior to hybridization to the array. The array was scanned with an iScan System (Illumina) and the data were analyzed using GenomeStudio Methylation Module Software (Illumina). A CpG site was considered to be informative if the sum of the signals for methylated and unmethylated sequences at the CpG site was significantly higher (at $P<0.05$) than signals of the negative control probes on the same array. Methylation levels were represented by β values, with a β value of 0 corresponding to no methylation and 1 corresponding to full methylation.

Quantitative methylation-specific PCR (qMSP). Sample DNA was treated with sodium bisulfite and purified as described previously (21). qMSP was performed using real-time PCR with bisulfite-modified DNA and specific primers (Table II, Fig. 1A). A methylation level was expressed as a percentage of the value of methylated DNA reference (PMR) calculated as the [(number of fragments methylated at a target locus in sample/number of the *Alu* sequences in sample)/(number of fragments methylated at a target locus in *Sss*I-treated DNA/ number of the *Alu* sequences in *Sss*I-treated DNA)]x100 (22).

Quantitative PCR following treatment with a methylation-dependent restriction enzyme (qPTMR). A fully unmethylated control was prepared by amplifying human blood genomic DNA with phi29 DNA polymerase (Illustra GenomiPhi HY kit, GE Healthcare, Buckinghamshire, UK) (23). DNA (1 μg) was treated with *Msp*JI (New England Biolabs, Beverly, MA, USA), which cleaves DNA 9 bp downstream from the ^{m}CNNR sequence (24,25), in a 30 μl reaction [4 U of *Msp*JI, 1X NEB buffer 4 (New England Biolabs) and 0.1 mg/ml BSA] at 37˚C for 20 h. Following purification, the DNA was treated with *Msp*JI again and dissolved in TE (10 mM Tris-HCl pH 8.0, 1 mM EDTA) at a concentration of 5 ng/μl without purification. Using 1 μl of the solution, quantitative PCR (qPCR) was performed by real-time PCR with primers that encompassed a target *Msp*JI site (Fig. 1B). To normalize the quantity of input DNA, the number of copies of a standard sequence, which may be amplified with a primer pair (5'-TTGCTTGAAGTTTTGTTGCTGTAGT-3' and 5'-AATAAACTCAGTTGTGACATGGACA-3') and contains no *Msp*JI site, was measured by qPCR. A percentage of the value of unmethylated reference (PUR) was calculated as the [(number of fragments at target locus in sample/number of the standard sequence in sample)/(number of fragments at target locus in GenomiPhi-amplified DNA/number of the standard sequences in GenomiPhi-amplified DNA)]x100. For convenience, the methylation level was expressed as 100-PUR.

Statistical analysis. Statistical analyses were conducted using PASW statistics version 18.0.0 (SPSS Japan Inc., Tokyo, Japan). The difference between the mean values of the two groups of samples was evaluated using Welch's t-test. The Fisher's exact test was used to evaluate the significant difference in relative frequency of the phenomena between two independent groups. Survival curves were computed according to the Kaplan-Meier method and the log-rank test was employed to evaluate the level of significant difference. $P<0.05$ was considered to indicate a statistically significant difference.

Results

Genome-wide screening using metastatic lymph nodes and GCs without LNM. To isolate the CpG sites that are hypermethylated specifically in GCs with LNM, genome-wide methylation analysis was performed using metastatic lymph nodes (n=3) and GCs without LNM (n=3) using an Infinium HumanMethylation450 BeadChip array. The samples used for this analysis were prepared from 6 patients in the screening

Table I. Clinicopathological data of sample sets.

	N	Age (years)	P-value	Gender	N	P-value	T stage	N	P-value
Genome-wide analysis set[a]									
Meta (-)	3	72±4	0.17	Male	2	1.0	T1	0	0.51
							T2	1	
				Female	1		T3	1	
							T4	1	
Meta (+)	3	59±13		Male	2		T1	0	
							T2	0	
				Female	1		T3	1	
							T4	2	
Screening set									
Meta (-)	10	69±6	0.13	Male	7	0.53	T1	0	0.17
							T2	1	
				Female	3		T3	6	
							T4	3	
Meta (+)	28	63±11		Male	18		T1	0	
							T2	0	
				Female	10		T3	14	
							T4	14	
Validation set									
Meta (-)	20	63±11	0.71	Male	13	0.6	T1	0	0.14
							T2	3	
				Female	7		T3	8	
							T4	9	
Meta (+)	129	62±10		Male	91		T1	0	
							T2	4	
				Female	38		T3	55	
							T4	70	

[a]This set comprised samples from the screening set.

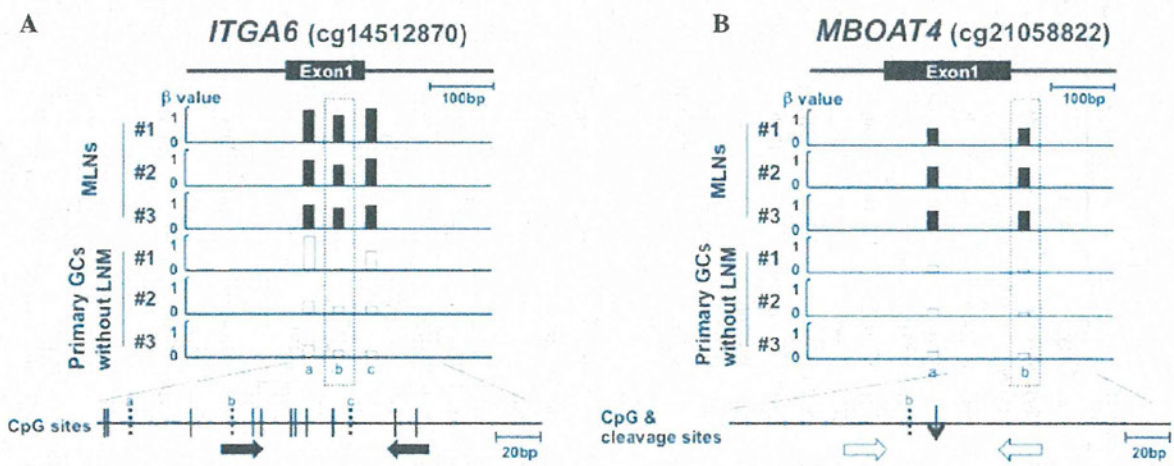

Figure 1. Representative genomic regions around the CpG sites differentially methylated between metastatic lymph nodes and GCs without LNM and primer design in the regions. Below the genomic structure of a region, β values (methylation levels) of the CpG sites carried by Infinium bead array are shown. The differentially methylated CpG site is marked by a rectangle with dotted line. A CpG map is drawn at the bottom, vertical lines (solid and broken lines) indicate CpG sites and broken lines indicate CpG sites whose β values were measured. (A) A region whose methylation level was assessed by qMSP. Primers specific to the methylated sequence (closed arrows) were designed on CpG sites around the differentially methylated sites based on the bisulfite-modified sequence. (B) A region whose methylation level was assessed by qPTMR. Primers (open arrows) were designed to amplify the region encompassing the *Msp*JI-cleaved site (thin vertical arrow) based on the unmodified sequence. GC, gastric cancer; MLN, metastatic lymph nodes; LNM, lymph node metastases; qMSP, quantitative methylation-specific PCR; qPTMR, quantitative PCR following treatment with a methylation-dependent restriction enzyme.

Table II. CpG sites identified by bead-chip array analysis.

No.	Probe name (IlmnID)[a]	Gene symbol	Location (Chr: base)	Relation to CpG island	Position to gene	P-value[b]		Cut-off (YI)	Primer sequences (5'-3')		Annealing temp.	PCR type	Mg^{2+c} (μM)
						Screening	Validation		Forward	Reverse			
1	cg23218354	-	Chr1: 2885244	Island	-	0.05	0.17	10.1 (0.48)	TGGTTTTTATACGGGGGATTTAC	ACTAAACCAAAACGACGATTACG	60	qMSP	1.5
2	cg13239126	*KIAA1026*	Chr1:15256136	-	Body	0.24	-	-	CTCCAGAGAGACAGGCATGGTT	CAAGCCTGACCTTCCCTCTCC	60	qPTMR	1.5
3	cg16112880	*TMEM9*	Chr1:201123745	Island	TSS200	0.41	-	-	CCCGCCCTCTCCTAGCTTCTAT	GGCTGACGTTCCCTTTTCTGGT	63	qPTMR	1.5
4	cg14512870	*ITGA6*	Chr2:173330342	-	Body	0.01	0.07	32.5 (0.44)	TATAGTTGCGATATTATCGTTC	AAACTACCGAAATAAACGCT	51	qMSP	2.5
5	cg09866366	*ABCF3*	Chr3:183903315	Shore	TSS1500	0.34	-	-	TCGTTAGATTACGGGTGTTTC	CAAAACGCATATATAACGATAACG	58	qMSP	2.5
6	cg08812108	-	Chr6:2515318	-	-	0.03	0.24	56.3 (0.44)	AGCGTTGGCGTTAGGTAGGGTAGTTC	CCAAATAACCACCTACGTCTTTACG	63	qMSP	1.5
7	cg06728252	*ABT1*	Chr6:26598149	Island	Body	0.24	-	-	CGCGTAGATCGGTTCGTGAGAC	GCCACGCGCTTAACTATACG	63	qMSP	1.5
8	cg08972588	*TNXB*	Chr6:32014674	-	Body	0.64	-	-	CCTGAGCAAGAATGAGGCCAGA	GGGGACAAGGGGGAGATCACA	65	qPTMR	2.5
9	cg22126965	*COX19*	Chr7:1015501	Shore	TSS1500	0.50	-	-	GGTTTAGAAAGGTTTAGCGAATTGTTC	AACAACCGCAAACAACG	62	qMSP	2.5
10	cg18450582	*DYNC1I1*	Chr7:95546539	-	Body	0.32	-	-	ACCTTGGCCTCTGGATTGTGGA	GCACTGCCTGCCTGAAAGGAGA	64	qPTMR	1.5
11	cg02005782	-	Chr7:105857664	-	-	0.59	-	-	GAAGTCAGCCAGGCATTGGAAG	CCCAGCTGCCTTTCTGATCTCT	65	qPTMR	1.5
12	**cg06436185**	*PRKAG2*	Chr7:151442351	-	Body	0.04	0.03	28.8 (0.24)	ATTTAGTTTTTTGTACGGTTGC	CCCAATAAAACGACGTAACG	55	qMSP	2.5
13	cg21058822	*MBOAT4*	Chr8:30002223	-	TSS200	0.38	-	-	GGCTGTCTCTGGTCTTTTTATC	AGAAAGCCAGTTTTTATTCTGC	61	qPTMR	1.5
14	cg12089032	-	Chr8:72881203	-	-	0.03	0.09	40.6 (0.41)	GCAAGTTAAGGCATCGTAGGAAAGC	GGCAGAGAGGAACAGCTCCTAAG	66	qPTMR	1.5
15	cg23170346	-	Chr8:134863880	-	-	0.95	-	-	CTAGCCACATCCATAGCAGACAGG	CACTCAGCAATGCAAACAGTCTTG	66	qPTMR	1.5
16	cg19878482	*C8orf73*	Chr8:144655026	Shore	TSS200	0.10	-	-	GGAGTTTTTCGGGTTCGGTTTC	CAAAAACCCATTATAAACACGTCCGT	65	qMSP	2.5
17	cg01263942	*DIP2C*	Chr10:695859	-	Body	0.01	0.12	23.2 (0.38)	GTTCGTTATTTGCGTTTTCGTGC	CAACGAAAAAACTCCATAAACCG	59	qMSP	2.5
18	cg03015672	*ARHGAP12*	Chr10:32216066	Shore	5'UTR	0.88	-	-	AGAACAGTGGAGCCGCATGCAA	CCAAAGCAGGCAGTGAAAGCGT	66	qPTMR	1.5
19	cg10326726	*MSMB*	Chr10:51549505	-	TSS200	0.16	-	-	CAACCCTCTGTAAACACTCAAT	TATAGACAGGTACATCCAGGCA	57	qPTMR	2.5
20	cg19864370	-	Chr10:80354592	-	-	0.00	0.29	70.6 (0.69)	GAATAGCTTAGGCCCCTGTCAT	GATAGTGCTAGCCCTTGGGAAT	60	qPTMR	1.5
21	cg03850986	*ABLIM1*	Chr10:116408382	-	Body	0.38	-	-	TGATAAAAATGCTCTGGAATTAG	TGGAGATGTAATGTAGTACACCATA	51	qPTMR	1.5
22	cg25885280	*SHANK2*	Chr11:70760166	-	Body	0.34	-	-	GCGGTGGGGGATTTCTGTAAGGA	GAGCAGGGTGTGCCTTCTCAGGG	68	qPTMR	1.5
23	cg26894278	*CRYL1*	Chr13:21016241	-	Body	0.22	-	-	GTTAAGTTTAAATGGAGCCTTG	TGACAGGATTACAATAAGGCTA	56	qPTMR	1.5
24	cg04339360	*KLF5*	Chr13:73635568	Shore	Body	0.04	0.31	25.4 (0.43)	TAGTCAAGAAAAGAAACCTGTGCAA	TGCCAAACTACCTCAATTCTGTTTA	61	qPTMR	1.5
25	cg16206504	-	Chr13:114917223	Shelf	-	0.02	0.35	35.2 (0.41)	CGAGATTGTAGGCGGTTGTTC	CCTAACTATTACAACAATACCGAACG	63	qMSP	1.5
26	cg14851578	-	Chr14:106187192	Shore	-	0.08	-	-	GGAGTGTGGGTTACGTGTGATTAC	CAATCTCGCCCACTCACG	66	qMSP	1.5
27	cg02990302	*C16orf80*	Chr16:58155189	-	Body	0.04	0.45	56.2 (0.65)	TCCTTTCCTTAGCTCCTTCCAG	AAAAACAGTCGGCTCTTTGTGA	63	qPTMR	1.5
28	cg08292959	*MGAT5B*	Chr17:74878420	Island	Body	0.97	-	-	GGCACCTGCCACTCCATCCG	TGCACTCTGGGCTGTACCACAGTG	63	qPTMR	1.5
29	cg15645685	*PBX4*	Chr19:19730175	Shore	TSS1500	0.26	-	-	CTAATGCTCCCTGCATCCTCAG	TAAACAAGCGAGGTCACTCTTCAGC	64	qPTMR	1.5
30	cg14571622	*NLRP8*	Chr19:56499348	-	3'UTR	0.01	-	-	TGGGGCTTGATTGATCAGTTCC	CCAGGGTTCAAAGCTGAGGTTC	62	qPTMR	1.5
31	cg27050343	*OTC*	ChrX:38211596	-	TSS200	0.15	-	-	AATTTTTGGGTTTAAGTGATTCGTTC	AAAAAAATAATTACTAACCGAACACG	62	qMSP	1.5

[a]IlmnID is a unique CpG site identifier from the Illumina CG database; underlined IlmnID indicates P<0.05 in the screening set; bold IlmnID, P<0.05 in the validation set. [b]Difference was evaluated by Welch's t-test. [c]Final concentration in a PCR analysis. Island, CpG island; Shore, within 2,000 bp of end of CpG island; Shelf, within 2,000 bp of end of Shore; TSS200, within 200 bp upstream of the transcription start site; TSS1500, 200-1,500 bp upstream of the TSS; 5'UTR, in the 5' untranslated region of the gene; Body, within exons or introns of the gene; 3'UTR, in the 3' untranslated region of the gene; YI, maximized Yoden index.

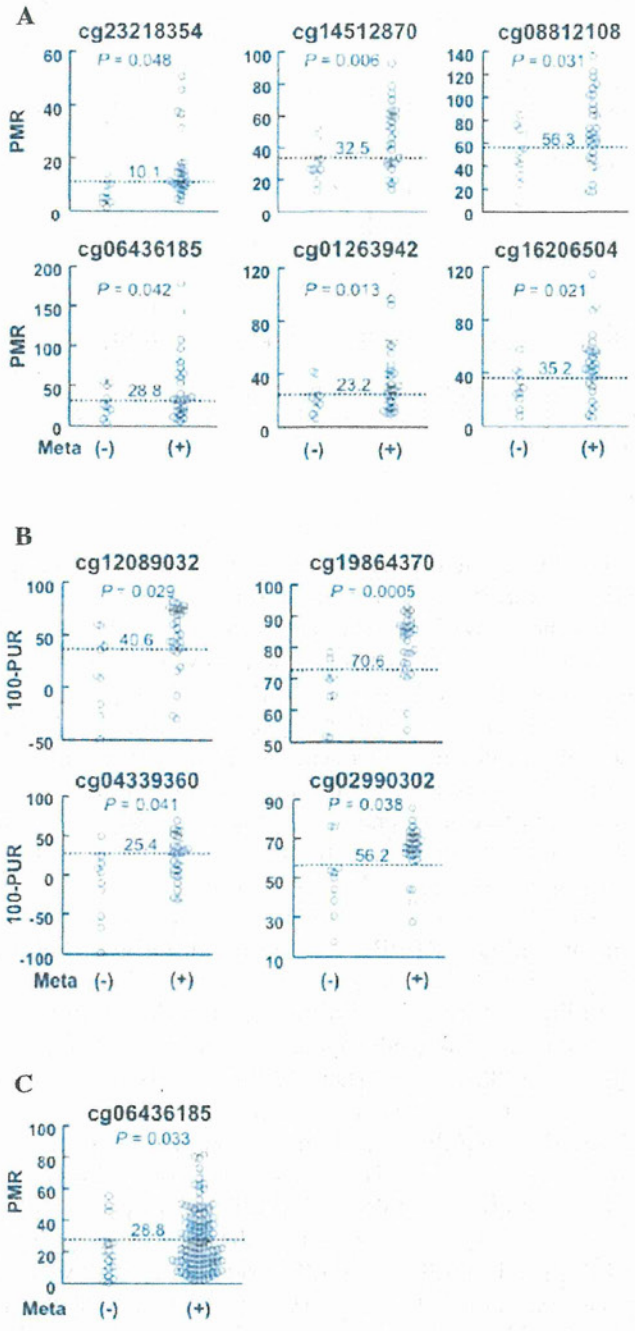

Figure 2. Methylation levels of the candidate genomic regions in primary GCs with and without LNM. Methylation levels were measured by (A) qMSP and (B) qPTMR in the screening sets. The screening set consisted of 10 GCs without LNM and 28 with LNM. (C) Methylation level of the region around cg06436185 in the validation sets was measured by qMSP. The validation set consisted of 20 GCs without LNM and 129 with LNM. Meta (-), GCs without LNM; Meta (+), those with LNM. Horizontal dotted lines are the cut-off methylation levels and the number on the line indicates the value of the level. GC, gastric cancer; LNM, lymph node metastases; qMSP, quantitative methylation-specific PCR; qPTMR, quantitative PCR following treatment with a methylation-dependent restriction enzyme; PUR, percentage of the value of unmethylated reference; PMR, percentage of the value of methylated DNA reference.

set (Table I). The mean number of informative CpG sites was 485,170 (SD 209) in the metastatic lymph nodes and 485,001 (SD 514) in the GCs without LNM (P=0.63). We searched for CpG sites that were highly methylated in the three metastatic lymph nodes [β value > a) 0.6, b) 0.5 and c) 0.4] and hardly

Table III. Association between methylation levels of the genomic region around cg0643618 and clinical characteristics.

		Methylation level		
Parameters	N	Mean	SD	P-value
Age				
≤60	77	32.2	24.0	0.26
>60	110	28.1	25.2	
Gender				
Female	58	34.9	26.4	0.07
Male	129	27.6	23.6	
T category				
T3	83	26.8	27.1	0.07
T4	96	33.6	22.5	

methylated in the three primary GCs without LNM (β value <0.2) and the number of hypermethylated CpG sites was a) 1, b) 31 and c) 209, respectively. To obtain a practicable number of candidate CpG sites, we adopted a cut-off β value of 0.5 and the 31 CpG sites were selected for further analysis (Table II).

Selection of informative candidate genomic regions among primary GCs. Using primary GCs with and without LNM (screening set, Table I), the methylation levels of genomic regions around the 31 CpG sites were measured by qMSP or qPTMR, which are accurate and sensitive enough to detect aberrant DNA methylation in a small population of cells. Of the 31 regions, 10 regions exhibited higher methylation levels in GCs with LNM (1.4- to 1.9-fold) than in those without LNM (Table II and Fig. 2A and B). For each of the 10 genomic regions, a cut-off methylation level was established in order that the Youden index (sensitivity + specificity - 1) would be maximized (Table II and Fig. 2).

Validation of the candidate genomic regions in a different set of samples. To validate the hypermethylation of the 10 candidate genomic regions in GCs with LNM, the methylation levels were analyzed in an independent sample set (validation set, Table I). A region around the cg06436185 CpG site revealed significantly higher methylation levels in GCs with LNM (1.5-fold) than those without (P=0.033, Fig. 2C), whereas the other nine regions were not validated (Table II). The region was located in the gene body of the *PRKAG2* gene and did not belong to a CpG island (Table II). Therefore, it was unlikely that the methylation status of the region around cg06436185 affected the transcription of a gene. Using a cut-off level established in the analysis of the screening set (28.8%), the presence of LNM was detected at a sensitivity of 43% and a specificity of 85%. This result indicated that a methylation level of this region is a candidate marker for the detection of the presence of LNM.

Association between the methylation level of the genomic region around the cg06436185 CpG site and clinicopathological characteristics. Associations between the methylation level of the genomic region around cg06436185

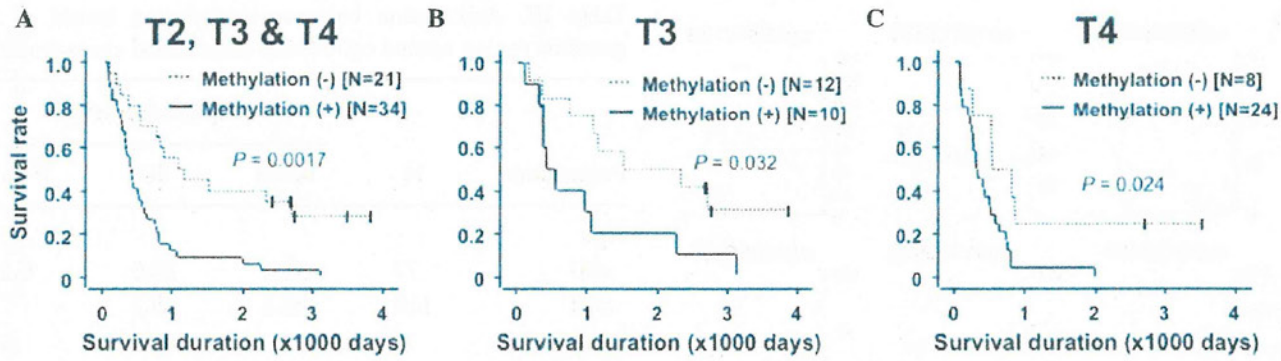

Figure 3. Kaplan-Meier analysis of 55 GC patients with LNM. (A) Overall survival in all the patients with LNM. (B and C) The survival curves of patients categorized into T3 and T4. Methylation (+), GCs with PMR of the region around cg06436185>28.8; Methylation (-), GCs with the PMR<28.8. GC, gastric cancer; LNM, lymph node metastases; PMR, percentage of the value of methylated DNA reference.

and clinicopathological characteristics (age, gender and T category) were analyzed in 157 GC patients with LNM and 30 without LNM. No difference in methylation levels according to age, gender or T category was found (Table III). Using 55 of the 157 GC patients with LNM, whose prognostic information was available (T2, one patient; T3, 22 patients; T4, 32 patients), a correlation between the methylation level and survival rate was analyzed. Patients with high methylation levels (>28.8%; the value used to detect the presence or absence of LNM) had a significantly poorer overall survival rate compared to those with low methylation levels (P=0.0017; Fig. 3A). Since the T category is known to be the major prognostic factor in GC patients (26), patients in the T3 and T4 categories were analyzed separately. In the T3 and T4 subgroups, the patients with high methylation levels demonstrated a significantly poorer overall survival rate than those with low methylation (P=0.032 and 0.024, respectively; Fig. 3B and C). These results revealed that the high methylation level of the genomic region around cg06436185 was associated with an unfavorable prognosis, regardless of the depth of tumor invasion.

Discussion

Using a genome-wide methylation analysis using metastatic lymph nodes and primary GCs without LNM, a genomic region (around cg06436185) whose methylation level in primary GCs was associated with the presence of LNM was successfully identified. Notably, the association was also significant in an independent validation set (P=0.033). Generally, markers isolated by genome-wide analyses need to be validated in a different set of samples due to the overfitting issues caused by multiple testing (27). Even in the present study, 9 of the 10 candidate genomic regions that revealed significant hypermethylation in GCs with LNM in the screening set (P=0.0005-0.048) were not reproduced in the validation set. This observation emphasizes the value of the methylation level of the genomic region around cg06436185. Since it had a sensitivity of 43% and specificity of 85%, the combined use of this novel methylation marker with imaging tools is predicted to improve the diagnostic accuracy of LNM of GCs.

The mean methylation levels of GCs with and without LNM were 18.7 and 27.5%. This small difference is extremely difficult to detect by a genome-wide screening method. Our strategy in the present study was to benefit from the monoclonal growth of cells in metastatic lymph nodes and compare metastatic lymph nodes and GCs without LNM. The methylation levels of the genomic regions around cg06436185 were 13.2 and 54.3%, respectively, in these samples. This relatively significant difference was identified using genome-wide screening, which has a relatively low accuracy in the analysis of methylation levels. Using a more accurate and sensitive method, qMSP, the small difference between GCs with and without LNM (18.7 and 27.5%, respectively) was clearly demonstrated.

A method to measure methylation levels in CpG-poor genomic regions, qPTMR, was developed using a combination of digestion with a methylation-dependent restriction enzyme and qPCR. qPTMR had an error range of 5% in this study. It is difficult to measure methylation levels in CpG-poor genomic regions by qMSP, a well-established method with a high accuracy, due to the difficulty in designing primers. Alternatively, *Msp*JI, a recently developed methylation-sensitive restriction enzyme, recognizes ^{m}CNNR (N=A, T, G or C; R=G or C) sequences and cleaves DNA when the C is methylated (24,25). Since the recognition sequence is applicable to the majority of CpG sites and cytosines in non-CpG sites are not methylated in somatic cells, the positive cleavage by *Msp*JI is used to determine methylation status of most CpG sites. Using qPTMR, the methylation levels of all the 19 candidate regions with few CpG sites were quantified. This new method is predicted to have various applications.

The methylation status of the genomic region around cg06436185 was unlikely to affect transcription of a known nearby gene (*PRKAG2*). However, its high methylation level in GCs, namely large fractions of cancer cells with methylation in cancer tissue, was associated with the presence of LNM and also with a poorer prognosis of the GC patients. One possible reason is that the region is located in a promoter region of unknown genes, including microRNA genes, or in enhancer regions whose methylation is critical for the regulation of gene expression levels. Another possible reason is that the methylation of the region is caused by an abnormality of unknown methylation regulation and that this abnormality is critical for tumor metsastasis or malignancy. In this case, other genomic regions are likely to be methylated in GCs with LNM or a poorer prognosis.

In conclusion, we identified one genomic region with a methylation status in primary GCs that was associated with the presence of LNM and a poorer prognosis of GC patients.

Acknowledgements

We thank Dr Michihiro Ishida, Dr Yukie Yoda and Dr Masahiro Maeda for their assistance during sample preparation. This study was supported by the Third-term Comprehensive Cancer Control Strategy from the Ministry of Health, Labour and Welfare, Japan, by the JSPS A3 Foresight Program and by the National Cancer Center Research and Development Fund. Y.S. is a recipient of Research Resident Fellowships from the Foundation for Promotion of Cancer Research.

References

1. Matsuda A and Matsuda T: Time trends in stomach cancer mortality (1950-2008) in Japan, the USA and Europe based on the WHO mortality database. Jpn J Clin Oncol 41: 932-933, 2011.
2. Kamangar F, Dores GM and Anderson WF: Patterns of cancer incidence, mortality, and prevalence across five continents: defining priorities to reduce cancer disparities in different geographic regions of the world. J Clin Oncol 24: 2137-2150, 2006.
3. Yokota T, Ishiyama S, Saito T, *et al*: Lymph node metastasis as a significant prognostic factor in gastric cancer: a multiple logistic regression analysis. Scand J Gastroenterol 39: 380-384, 2004.
4. Chen JH, Wu CW, Lo SS, *et al*: Lymph node metastasis as a single predictor in patients with Borrmann type I gastric cancer. Hepatogastroenterology 54: 981-984, 2007.
5. Saito H, Fukumoto Y, Osaki T, *et al*: Prognostic significance of level and number of lymph node metastases in patients with gastric cancer. Ann Surg Oncol 14: 1688-1693, 2007.
6. Sano T and Aiko T: New Japanese classifications and treatment guidelines for gastric cancer: revision concepts and major revised points. Gastric Cancer 14: 97-100, 2011.
7. Bonenkamp JJ, Songun I, Hermans J, *et al*: Randomised comparison of morbidity after D1 and D2 dissection for gastric cancer in 996 Dutch patients. Lancet 345: 745-748, 1995.
8. Cuschieri A, Fayers P, Fielding J, *et al*: Postoperative morbidity and mortality after D1 and D2 resections for gastric cancer: preliminary results of the MRC randomised controlled surgical trial. The Surgical Cooperative Group. Lancet 347: 995-999, 1996.
9. Degiuli M, Sasako M, Ponti A, Soldati T, Danese F and Calvo F: Morbidity and mortality after D2 gastrectomy for gastric cancer: results of the Italian Gastric Cancer Study Group prospective multicenter surgical study. J Clin Oncol 16: 1490-1493, 1998.
10. Seevaratnam R, Cardoso R, McGregor C, *et al*: How useful is preoperative imaging for tumor, node, metastasis (TNM) staging of gastric cancer? A meta-analysis. Gastric Cancer: Aug 12, 2011 (E-pub ahead of print).
11. Ganpathi IS, So JB and Ho KY: Endoscopic ultrasonography for gastric cancer: does it influence treatment? Surg Endosc 20: 559-562, 2006.
12. Yoshioka T, Yamaguchi K, Kubota K, *et al*: Evaluation of ^{18}F-FDG PET in patients with advanced, metastatic, or recurrent gastric cancer. J Nucl Med 44: 690-699, 2003.
13. Ha TK, Choi YY, Song SY and Kwon SJ: F18-fluorodeoxyglucose-positron emission tomography and computed tomography is not accurate in preoperative staging of gastric cancer. J Korean Surg Soc 81: 104-110, 2011.
14. Natsugoe S, Mueller J, Stein HJ, Feith M, Hofler H and Siewert JR: Micrometastasis and tumor cell microinvolvement of lymph nodes from esophageal squamous cell carcinoma: frequency, associated tumor characteristics, and impact on prognosis. Cancer 83: 858-866, 1998.
15. Kojima N, Yonemura Y, Bando E, *et al*: Optimal extent of lymph node dissection for T1 gastric cancer, with special reference to the distribution of micrometastasis, and accuracy of preoperative diagnosis for wall invasion. Hepatogastroenterology 55: 1112-1117, 2008.
16. Motoyama K, Inoue H, Mimori K, *et al*: Clinicopathological and prognostic significance of PDCD4 and microRNA-21 in human gastric cancer. Int J Oncol 36: 1089-1095, 2010.
17. Tanaka M, Kitajima Y, Edakuni G, Sato S and Miyazaki K: Abnormal expression of E-cadherin and beta-catenin may be a molecular marker of submucosal invasion and lymph node metastasis in early gastric cancer. Br J Surg 89: 236-244, 2002.
18. Arigami T, Natsugoe S, Uenosono Y, *et al*: CCR7 and CXCR4 expression predicts lymph node status including micrometastasis in gastric cancer. Int J Oncol 35: 19-24, 2009.
19. Shen Z, Ye Y, Dong L, *et al*: Kindlin-2: a novel adhesion protein related to tumor invasion, lymph node metastasis, and patient outcome in gastric cancer. Am J Surg 203: 222-229, 2012.
20. Bibikova M, Barnes B, Tsan C, *et al*: High density DNA methylation array with single CpG site resolution. Genomics 98: 288-295, 2011.
21. Oka D, Yamashita S, Tomioka T, *et al*: The presence of aberrant DNA methylation in noncancerous esophageal mucosae in association with smoking history: a target for risk diagnosis and prevention of esophageal cancers. Cancer 115: 3412-3426, 2009.
22. Niwa T, Tsukamoto T, Toyoda T, *et al*: Inflammatory processes triggered by *Helicobacter pylori* infection cause aberrant DNA methylation in gastric epithelial cells. Cancer Res 70: 1430-1440, 2010.
23. Niwa T, Yamashita S, Tsukamoto T, *et al*: Whole-genome analyses of loss of heterozygosity and methylation analysis of four tumor-suppressor genes in N-methyl-N'-nitro-N-nitrosoguanidine-induced rat stomach carcinomas. Cancer Sci 96: 409-413, 2005.
24. Zheng Y, Cohen-Karni D, Xu D, *et al*: A unique family of Mrr-like modification-dependent restriction endonucleases. Nucleic Acids Res 38: 5527-5534, 2010.
25. Cohen-Karni D, Xu D, Apone L, *et al*: The MspJI family of modification-dependent restriction endonucleases for epigenetic studies. Proc Natl Acad Sci USA 108: 11040-11045, 2011.
26. Yokota T, Ishiyama S, Saito T, *et al*: Is tumor size a prognostic indicator for gastric carcinoma? Anticancer Res 22: 3673-3677, 2002.
27. Simon R, Radmacher MD, Dobbin K and McShane LM: Pitfalls in the use of DNA microarray data for diagnostic and prognostic classification. J Natl Cancer Inst 95: 14-18, 2003.

Digestive Endoscopy
Journal for Gastroenterologists and Endoscopic Surgeons

Digestive Endoscopy (2012) **24**, 110–116 doi:10.1111/j.1443-1661.2011.01178.x

ORIGINAL ARTICLE

PROSPECTIVE SINGLE-ARM TRIAL OF TWO-WEEK RABEPRAZOLE TREATMENT FOR ULCER HEALING AFTER GASTRIC ENDOSCOPIC SUBMUCOSAL DISSECTION

Keiko Niimi,[1] Mitsuhiro Fujishiro,[2] Osamu Goto,[1] Shinya Kodashima,[3] Chihiro Minatsuki,[1] Itsuko Hirayama,[1] Satoshi Mochizuki,[1] Satoshi Ono,[1] Nobutake Yamamichi,[1] Naomi Kakushima,[4] Masao Ichinose[5] and Kazuhiko Koike[1]

Departments of [1]Gastroenterology and [2]Endoscopy and Endoscopic Surgery, Graduate School of Medicine, The University of Tokyo, [3]Center for Epidemiology and Preventive Medicine, The University of Tokyo, Tokyo, [4]Endoscopy Division, Shizuoka Cancer Center, Shizuoka and [5]Second Department of Internal Medicine, Wakayama Medical University, Wakayama, Japan

Aim: Endoscopic submucosal dissection (ESD) causes artificial ulcers, and there is no consensus regarding the degree of healing in ESD-induced ulcers or the optimal duration of proton pump inhibitor (PPI) treatment. The aim of the present study was to investigate the healing rates of post-ESD ulcers in response to the protective effect of 2-week PPI treatment.
Methods: Between February 2007 and March 2010, 75 patients/75 lesions and 55 patients/55 lesions were enrolled as interim and per-protocol groups, respectively. All patients were prescribed rabeprazole (10 mg/day) orally for 16 days beginning on the day before ESD. Follow-up endoscopy was carried out 8 weeks after ESD to evaluate ulcer healing. The primary end-point was the healing rate of post-ESD ulcers at 8 weeks after ESD. Secondary end-points were the rate of post-ESD bleeding with emergency endoscopy and the rate of other severe adverse effects during the study period.
Results: The transitional rate to scarring-stage ulcers was 80.0% (44/55). Location in the lesser curve and large resected size (>40 mm) were statistically significant predictors for delayed ulcer healing by univariate analysis and the latter was still significant by the multivariate analysis. Post-ESD bleeding occurred within 2 weeks in two cases (2.7%), but both cases were successfully managed with endoscopic hemostasis only. Severe adverse effects did not occur.
Conclusions: Two-week administration of PPI for post-ESD gastric ulcers may be sufficient to aid healing without increasing any adverse effects in cases where there are no possible deteriorating factors on ulcer healing, although large resection and/or resection in the lesser curve may result in delayed healing even after 8 weeks of ESD.

Key words: endoscopic submucosal dissection, gastric intraepithelial neoplasm, postoperative bleeding, proton pump inhibitor, ulcer healing.

INTRODUCTION

After the recognition of *Helicobacter pylori* (*H. pylori*) and several non-steroidal anti-inflammatory drugs (NSAIDs) as causative factors of ulcers, the pathogenesis of gastric ulcer diseases has been studied mainly from these two major etiological categories.[1–4] The recommended treatment strategies for gastric ulcer diseases are *H. pylori* eradication, cessation of NSAIDs, cyclooxygenase (COX)-2 inhibitors, antisecretory drugs and prostaglandin analogs with NSAIDs, depending on the case.[5,6]

Early exposure to gastroscopy to detect curable gastric neoplasia, as a nationwide gastric cancer screening program, has rapidly increased the number of endoscopic resections for these lesions, especially in Asian countries.[7] The chronological trend in the number of operations for early gastric cancers (EGC) at National Cancer Center Hospital, Tokyo, Japan, reveals that the number of endoscopic resections exceeded that of surgical gastrectomies from 2001.[8] As a new category of gastric ulcer diseases, an artificial ulcer after endoscopic resection (e.g. endoscopic mucosal resection [EMR] and endoscopic submucosal dissection [ESD]) has attracted its own field of study. However, little is known about artificial ulcers, especially ESD, and so far they have been treated as similar to *H. pylori*-negative and NSAID-negative peptic ulcers.[6] Therefore, they are treated with proton pump inhibitors (PPI) for approximately 8 weeks after ESD in most hospitals.[9,10]

In a previous preliminary case series, we found that 8 weeks of PPI and sucralfate seemed to be sufficient to cure even a large ESD ulcer when the treated tumors had no submucosal fibrosis.[11,12] In cases of EMR, Lee *et al.* reported that treatment with PPI for 1 week was equivalent to treatment for 4 weeks in terms of ulcer reduction ratio or ulcer stage at 4 weeks after EMR, although the created ulcer size was approximately 2 cm in diameter.[13] This finding suggests that artificial ulcers caused by endoscopic resection might heal faster than *H. pylori*- or NSAID-related peptic ulcers,

Correspondence: Mitsuhiro Fujishiro, Department of Endoscopy and Endoscopic Surgery, Graduate School of Medicine, The University of Tokyo, 7-3-1 Hongo, Bunkyo-ku, Tokyo 113-8655, Japan. Email: mtfujish-kkr@umin.ac.jp

Received 15 January 2011; accepted 02 May 2011.

even if the larger artificial ulcer is created by ESD, and spontaneous healing might be expected after postoperative bleeding complications are successfully managed. Several studies have revealed that postoperative bleeding occurs frequently within 24 h and, at the latest, 7 to 10 days after ESD.[10,14–16] Therefore, we prospectively evaluated the healing rate of post-ESD ulcers and the factors influencing delayed healing by 2-week PPI therapy at index endoscopy carried out 8 weeks after ESD.

METHODS

Study design

The present study was a single-arm prospective trial. The study protocol was approved by the institutional review board (IRB) of the University of Tokyo Hospital, Tokyo, Japan, and was registered in the University hospital Medical Information Network Clinical Trials Registry (UMIN-CTR) as number UMIN000000688. There was no pharmaceutical industry support for this study. The authors vouch for the completeness and veracity of the data and data analyses.

Patients

Patients were enrolled in this study if they were scheduled to undergo ESD for gastric epithelial neoplasms at the University of Tokyo Hospital, Tokyo, Japan, between February 2007 and March 2010 after receiving IRB approval for this study. ESD became one of the treatment options for lesions with preoperative diagnosis of gastric adenoma or possible node-negative EGC: intramucosal intestinal-type cancer without ulcerative findings, regardless of size (M-UL[–]); intramucosal intestinal-type cancer with ulcerative findings, 3 cm or less in size (M-UL[+]); or intestinal-type cancer with slight submucosal invasion of less than 500 μm from the muscularis mucosae, 3 cm or less in size (SM1).[17] Patients were informed of the risks and benefits of several treatments, including ESD, conventional EMR, ablation therapy, and surgical gastrectomy.

Among all the patients who provided written informed consent for ESD, patients with any of the following were excluded from the study: concomitant administration of antithrombotic agents, corticosteroids or NSAIDs; drug allergy to PPI; severe comorbidity (i.e. liver cirrhosis, renal failure, or respiratory failure); multiple primary lesions that caused more than one post-ESD ulcer; or lesions with ulcerative findings.[18–20] Lesions with ulcerative findings were exclusion criteria because our previous study revealed that ulcerative lesions delayed artificial ulcer healing even if PPI and sucralfate were given for 8 weeks.[12]

Interim registration was permitted for the patients who provided written informed consent for participation in this study according to Good Clinical Practice guidelines, and final registration was 2 weeks after ESD, when histopathological diagnosis of the resected specimens was obtained and rabeprazole administration for 2 weeks after ESD was completed, without severe perioperative complications, such as perforation or massive bleeding. Patients with histopathological diagnoses potentially requiring additional treatment were excluded from the final registration as follows: SM2 (massive submucosal invasion of more than 500 μm from the muscularis mucosae) or deeper; vessel infiltration; diffuse-type neoplasia; or tumor exposure on the vertical or horizontal margins of the resected specimens. Lesions with ulcerative findings by histological evaluation were also excluded because of possible delays in ulcer healing, as previously described.[12]

Study protocol

The bleeding rates of post-ESD were 3.4% (13/383) in our previous case series and 6.1% (59/945) in another leading center,[14,21] and all bleeding events occurred within 2 weeks after ESD. Therefore, we considered 2 weeks of PPI necessary and sufficient to prevent postoperative bleeding. Patients were prescribed 10 mg oral rabeprazole daily from the day before ESD to the 14th day after ESD. Other antisecretory drugs that may promote ulcer healing and NSAIDs, including aspirin, which may diminish ulcer healing, were prohibited until 8 weeks after ESD, when the second follow-up (index) endoscopy was carried out.

ESD was carried out as previously reported.[22–24] In brief, the procedure consisted of marking around the lesion, injection into the submucosal layer, mucosal incision around the marking, and submucosal dissection beneath the lesion. Submucosal injection solution, endosurgical knives and other equipment were not predetermined for this study but were selected by the operators based on their experience and the characteristics of the lesions. Perioperative patient care, except for administration of antisecretory drugs, was standard.[16] Patients without complications were usually allowed to eat a light meal the day after ESD.

The first follow-up endoscopy was carried out once within a week to check whether there was a recent hemorrhage or a possible bleeding spot that should be treated on the post-ESD ulcer. The day of the first follow-up endoscopy was decided by the operator according to the patient's condition. When bleeding or non-bleeding visible vessels were seen (sometimes in removing adherent clots by forceps or water jet) during the endoscopy, prophylactic hemostasis was carried out. Clipping with hemostatic clips (HX-610–135 or HX-610–090L; Olympus, Tokyo, Japan) was carried out for large non-bleeding vessels, and thermocoagulation with hemostatic forceps was carried out for bleeding vessels or small non-bleeding vessels or in locations where it was difficult to place a clip because of consolidation of the ulcer bed. If the hospitalization was uneventful, patients were discharged within 1 week after ESD.

Post-ESD bleeding was defined when emergency endoscopy because of apparent hematemesis or melena, changes of vital signs, and/or progressive anemia (e.g. a rapid fall in hemoglobin level of 2 g/dL or more) revealed a post-ESD ulcer with evidence of recent or ongoing bleeding. The patients with post-ESD bleeding were treated with the best available endoscopic hemostasis and supportive tools.

Index endoscopy was carried out at 8 weeks after ESD to evaluate the healing process of the ulcer and to check whether there was a recent hemorrhage or a possible bleeding spot. Patients were advised to contact the doctor in charge in case of hematemesis or melena, even after discharge. The ulcer-healing stage was evaluated using the six-stage classification known as "Sakita-Miwa classification",[25] and ulcer healing

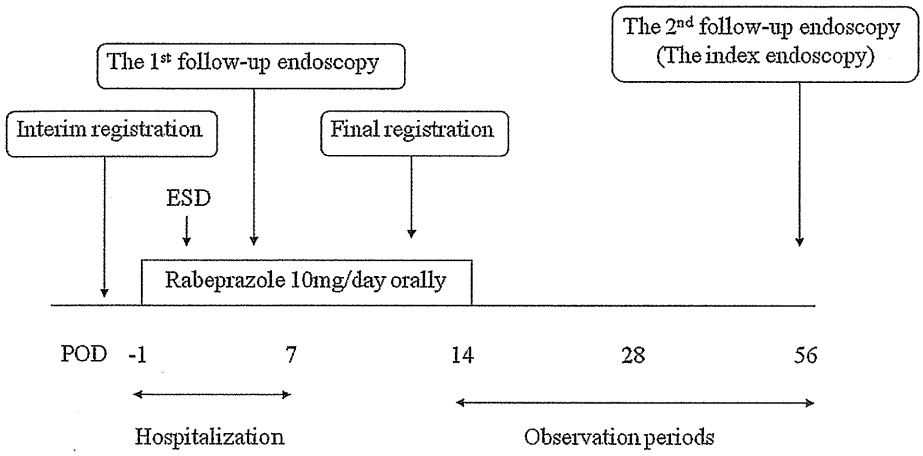

Fig. 1. Treatment protocol. POD, post-operative day.

was defined as reaching the S1 stage. Patients completed the study period at index endoscopy, and additional management was left to the doctors in charge (Fig. 1).

End-points

Our primary end-point was the healing rate of post-ESD ulcers at 8 weeks after ESD among the finally registered patients. Secondary end-points included the rate of post-ESD bleeding with emergency endoscopy and the rate of other severe adverse effects during the study period in all preregistered patients.

Sample size

We did not make a control arm for this study because we had already reported that the healing rate of post-ESD ulcers by giving PPI and sucralfate for 8 weeks was 100% (95/95) as a historical control from our preliminary study. Additionally, the healing rates of peptic ulcers by giving PPI for 6 to 8 weeks have been reported to be more than 80%, which is clinically acceptable for gastric ulcer treatment.[26] Therefore, we considered it clinically acceptable if 2-week administration of rabeprazole resulted in a >80% healing rate at 8 weeks after ESD. Assuming that 90% of our patients healed at 8 weeks after ESD by 2-week administration of rabeprazole, which was 10% higher than the acceptable level, the required number of patients was 34. Additionally, when post-ESD bleeding was considered to determine the sample size with a statistical power of 95%, the required number of patients was 50, assuming 6% of our patients had post-ESD bleeding. We therefore aimed to recruit 55 patients for a valid analysis.

Statistical analysis

Statistical analysis was carried out using JMP version 8.0 software (SAS Institute, Cary, NC, USA). Patient data were statistically compared by using the chi-squared test for categorical data and Student's *t*-test for numerical data as univariate analysis. *P*-values less than 0.05 were considered significant. If there was more than one predictor with a significant difference by univariate analysis, multivariate analysis was carried out. Predictors with *P*-values less than 0.2 by univariate analysis were included in multivariate analysis using a stepwise logistic regression model.

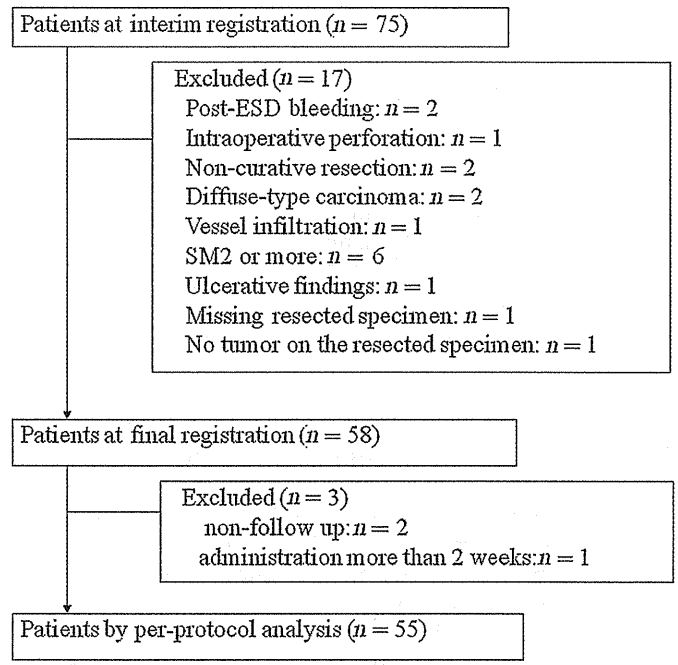

Fig. 2. Flowchart of the participants.

RESULTS

Between February 2007 and March 2010, 75 patients/75 lesions and 58 patients/58 lesions were enrolled as the interim group and the final group, respectively (Fig. 2). Seventeen patients/17 lesions were excluded from the final registration for the following reasons: two for post-ESD bleeding within 2 weeks, one for intraoperative perforation, two for non-curative resection, two for diffuse-type carcinoma, one for vessel infiltration, six for SM2 invasion, one for ulcerative findings, one for lack of the resected specimen before retrieving from the stomach, and one for no tumor on the resected specimen. Among 58 patients/58 lesions in the final group, two patients did not visit our hospital for the index endoscopy, one patient took rabeprazole

Table 1. Demographic and clinicopathological characteristics of patients in the current study†

	75 patients	55 patients
Age, mean (range), years	67.1 (41–85)	67.9 (50–85)
Sex (Female/Male)	24/51	17/38
Smoking (Yes/No)	18/57	14/41
Alcohol (Yes/No)	37/38	25/30
Helicobacter pylori (positive/negative)	48/27	35/20
Diabetes mellitus (Yes/No)	8/67	4/51
Hypoalbuminemia (Yes/No)	4/71	3/52
Lesion size, mean (range), mm	18.6 (1–120)	17.2 (1–60)
<10/–20/–30/–40/–50/–60/61< , mm	26/27/11/4/4/1/2	20/18/10/3/2/2/0
Location (U/M/L)	15/35/25	15/24/16
Circumference (AW/GC/LC/PW)	13/9/27/26	7/7/22/19
Macroscopic type		
Protruded type (0–I, 0–IIa)	26	19
Depressed type (0–IIc)	46	33
Flat type (0–IIb)	3	3
Tumor depth		
Adenoma	2	1
M	56	48
SM1	8	6
SM massive	6	0
Unknown	3	0
En bloc resection (Yes/No)	72/3	52/3
Resected size, mean (range), mm	33.9 (14–134)	32.7 (15–73)
Procedure time, mean (range), min	94.8 (20–230)	91.3 (20–220)

†75 patients/75 lesions in the interim group and 55 patients/55 lesions in the per-protocol analysis.
AW, anterior wall; GC, greater curve; L, lower third; LC, lesser curve; M, middle third; PW, posterior wall; SM1, minimally invasive carcinoma with infiltration depth ≦500 μm; U, upper third.

more than 2 weeks after ESD by mistake, and 55 patients/55 lesions could be investigated as the per-protocol analysis.

Table 1 summarizes the baseline demographic and clinicopathological characteristics of 75 patients/75 lesions in the interim group and 55 patients/55 lesions in the per-protocol analysis. *H. pylori* status was evaluated by either serological testing or urea breath test. Procedure time was measured from marking to the end of tumor removal. Histology was unknown in three lesions because of lack of resected specimen, no tumor on the resected specimen, and severe burn effect of the resected specimen. In order to investigate the predictors for delayed healing as a post-hoc analysis, we divided patients into two groups for each possible parameter.

Primary end-point

Among 55 valid ulcers for the per-protocol analysis of ulcer healing, 11 and 44 improved to H2 stage and S1 stage, respectively, at 8 weeks after ESD. The transitional rate to ulcer scar was 80.0% (44/55). Circumferential location (lesser curve *vs* others) and resected size (≦40 mm *vs* 40< mm) were significantly associated with differences in ulcer healing at 8 weeks by univariate analysis (Tables 2,3). When we carried out logistic multivariate analysis using seven possible variables derived by univariate analysis, only the resected size was statistically significant (odds ratio, 6.26; 95% confidence interval, 1.36–32.10; $P = 0.0207$). The third follow-up endoscopy was carried out for 33 of the 55 patients. During the follow-up period (mean, 10.3 months; range, 4–16 months), all post-ESD ulcers improved to S1 stage without additional administration of PPI, which included six H2-stage ulcers at the index endoscopy.

Table 2. Post-ESD ulcer healing stage at 8 weeks, according to patient factors

	H2 stage	S1 stage	*P*-value
Age			0.3153
≦70 years	4	25	
>70 years	7	19	
Sex			0.2858
Male	6	32	
Female	5	12	
Smoking			0.8820
Yes	3	11	
No	8	33	
Alcohol			0.3262
Yes	3	22	
No	8	22	
Diabetes mellitus			0.1748
Yes	2	2	
No	9	42	
Hypoalbuminemia			0.4952
Yes	1	2	
No	10	42	
Helicobacter pylori			0.1810
Positive	5	30	
Negative	6	14	

ESD, endoscopic submucosal dissection.

Table 3. Post-ESD ulcer healing stage at 8 weeks, according to lesion characteristics

	H2 stage	S1 stage	*P*-value
Lesion diameter			0.1607
≤20 mm	5	31	
>20 mm	6	13	
Resected diameter			0.0017
≤40 mm	4	38	
>40 mm	7	6	
Location			0.6097
U	4	11	
M	5	19	
L	2	14	
Circumference			0.0186
LC	8	14	
Others: GC	0	7	
AW	0	7	
PW	3	16	
Histological depth			0.3669
Adenoma	0	1	
M	11	37	
SM1	0	6	
Macroscopic type			0.2338
Protruded type (0–I, 0–IIa)	2	17	
Depressed type (0–IIc)	9	24	
Flat type (0–IIb)	0	3	
En bloc resection			0.0985
Yes	9	43	
No	2	1	
Procedure time			0.1607
≤90 min	5	31	
>90 min	6	13	

AW, anterior wall; ESD, endoscopic submucosal dissection; GC, greater curve; L, lower third; LC, lesser curve; M, middle third; PW, posterior wall; SM1, minimally invasive carcinoma with infiltration depth ≤500 μm; U, upper third.

Secondary end-point

The first follow-up endoscopy of 75 lesions in the interim group was carried out for 74 lesions (median, 1 day after ESD; range, 1–8 days), excluding one case of postoperative bleeding before the first follow-up endoscopy. Prophylactic hemostasis for bleeding or non-bleeding visible vessels during the endoscopy was carried out for 18/74 lesions (24.3%), according to the judgment of the endoscopist in charge. Overall rates of perforation and postoperative bleeding requiring emergency endoscopy were 1.3% (1/75) and 2.7% (2/75), respectively, and these bleeding complications occurred on 2 days and 7 days after ESD, respectively. The former occurred before the first follow-up endoscopy, and the latter occurred after the first follow-up endoscopy without prophylactic hemostasis. No patients needed emergency surgery for complications or blood transfusions for massive bleeding. In the 55 patients in the per-protocol analysis, post-ESD bleeding with emergency endoscopy and severe adverse effects did not occur.

DISCUSSION

The present study is the first prospective study showing that PPI treatment for 2 weeks after gastric ESD may be sufficient for post-ESD ulcers to heal, when the patients have no severe comorbidities and no concomitant use of possible ulcer-promoting drugs and the target lesions have no submucosal involvement, such as ulcerative findings or deep tumor invasion.[12] These results are meaningful not only for the possibility of reducing the cost of post-ESD management but also for understanding the differences between the healing processes of peptic ulcers and artificial ulcers.

In our preliminary observational study using endoscopy, ESD ulcers under 8-week PPI and sucralfate administration were covered by a white mucoid cap at 1 week, followed by reduction to almost half of the initial size by 4 weeks. There was a slight appearance of regenerative mucosa at the border at 4 weeks, and the remaining mucosal defect was fully covered by 8 weeks, regardless of resected size or location.[11] Another study using the surgically resected specimens after gastric ESD revealed that the mechanism of size reduction of these ulcers was contraction of the ulcer for the first few weeks, followed by slow coverage by regenerative mucosa. The remarkable contraction was assumed to be due to the contraction of the intact proper muscle layer.[27] Enhancement of gastric mucosal blood flow at the ulcer margin is an important factor for mucosal regeneration and Hashimoto *et al.* found that blood flow at the margin of EMR-induced ulcer was higher compared with that in a corresponding area of peptic ulcers, the latter being more prone to relapse.[28,29] These findings suggest that artificial ulcer after EMR or ESD may have a more self-healing process.

In addition, the present study showed that the healing process could spontaneously continue without the help of PPI at least as early as 2 weeks after ESD. There is no clear reason for the cut-off time of 2 weeks in terms of the healing effect of PPI, but we speculated that the most serious complications after ESD were postoperative bleeding and perforation which may occur within 2 weeks after ESD. So, it is still controversial to set the length of PPI for a shorter duration (e.g. 1 week), similar to that of EMR.[13] In terms of ulcer-related symptoms, we did not investigate them in detail, because Lee *et al.* reported that no significant differences in ulcer-related symptoms at 4 weeks after EMR were observed between the 1-week PPI group and the 4-week PPI group.[13] In fact, we did not get any complaints from the participating patients requesting painkillers during the study period.

Before the role of *H. pylori* was known, the multifactorial pathogenesis of gastric ulcer had been studied mainly from the perspective of an imbalance of aggressive gastric luminal factors (acid and pepsin) and defensive mucosal barrier function (mucus and local mucosal blood flow).[30] According to the imbalance theory, aggressive factors are heavily suppressed in the gastric environment where gastric cancer emerges because atrophic gastritis with low acidity and low pepsin production pre-exists in most patients with gastric cancer, as a precancerous condition. Thus, the healing efficacy of acid suppression by PPI may be limited in cases of post-ESD ulcers.

However, the efficacy of PPI for post-ESD bleeding has to be considered as a different clinical entity from that for ulcer healing. A few studies have investigated the risk factors of post-ESD bleeding: large tumor size (e.g. >2 cm), scar in the tumor, and middle or lower tumor location.[9,10,31] When the target lesion is small, without a scar, and located in the upper stomach, shorter PPI therapy may be acceptable from both aspects of post-ESD bleeding and ulcer healing.

In the present study, not all of the post-ESD ulcers healed at 8 weeks after ESD, although an additional endoscopy 8 weeks or more after ESD revealed ulcer healing without any specific medication in the non-healing cases. When we consider that the clinical significance of achieving ulcer healing may be to relieve any adverse effects and prevent bleeding from the created ulcer, the obtained healing effect, without any significant adverse effects or any post-ESD bleeding later than 14 days after ESD in this study, must be acceptable in daily practice. In our post-hoc analysis to investigate the predictors related to delayed healing under preconditioning of this study with no deteriorating factors on ESD ulcer healing, location of the lesser curve and large resected size (>40 mm) were significant by univariate analysis and large resected size was still only a predictor by multivariate analysis.

In terms of location, the theory of a dual-control mechanism of ulcer formation, as effected by the mucosa and musculature of the stomach, which was established in 1969 by Oi *et al.*,[32] might explain the possible reason. In agreement with the dual-control mechanism, nearly all gastric ulcers were located adjacent to a mucosal boundary on the side opposite the fundic gland area in relation to the gastric mucosa and/or were located within identifiable special muscular areas where oblique muscle bundles were lacking in relation to the gastric musculature. The latter existed at the narrow lesser curvature of the corpus of the stomach, and gastric motility creates severe kinetic strain in this area. Thus, in case of the lesser curve, the shorter duration of PPI could not counterbalance the negative force for ulcer healing in relation to the gastric musculature. In terms of the resected size, it is quite reasonable for the larger ulcer to need more time for healing. Even in both conditions, however, it is still controversial to use PPI for a longer duration, because there was no adverse effect on patients with delayed healing by 2 weeks of PPI treatment.

After *H. pylori* had been known to be an important factor in healing of peptic ulcer, eradication of *H. pylori* has been recommended to prevent peptic ulcer recurrence. Moreover, Fukase *et al.* reported that eradication of *H. pylori* after endoscopic resection of EGC resulted in an odds ratio of 0.353 for metachronous gastric cancer in comparison with non-eradication in the following 3 years.[33] Although eradication of *H. pylori* should be considered to lessen a metachronous gastric cancer, it may be unnecessary to eradicate it in order to lessen artificial ulcer recurrence, because the pathogenesis is completely mechanical, not due to degradation of gastric mucosa by gastric juice or apoptosis by *H. pylori* and this study also revealed no significant effect on delayed healing.

The major limitation of the present study is that patients with concomitant use of possible ulcer-promoting drugs were excluded. Antithrombotic agent usage has been increasing recently and our consecutive cases of gastric ESD between January 2000 and December 2007 revealed that 11.5% of them were receiving antithrombotic agents.[34]

Patients with ulcerative findings in the tumor were also excluded due to possible delayed healing. When delayed healing does not cause any significant events for the patients, however, these patients may be managed similarly to patients without ulcerative findings (i.e. 2 weeks of PPI administration). Further studies are necessary to determine the appropriate administration of PPI or whether another ulcer-healing drug is better for these patients, from the aspects of both post-ESD bleeding and ulcer healing.

In conclusion, this study revealed that 2-week administration of PPI for post-ESD gastric ulcers may be effective and sufficient to help them heal without increasing any adverse effects in cases where there are no deteriorating factors on ESD ulcer healing. Taken together, our results indicate that artificial ulcers caused by endoscopic resection may be categorized as a new entity of gastric ulcer disease and that their healing process and management should be investigated differently from peptic ulcer disease in some respects.

REFERENCES

1. Treiber G, Lambert JR. The impact of *Helicobacter pylori* eradication on peptic ulcer healing. *Am. J. Gastroenterol.* 1998; **93**: 1080–4.
2. Arkkila PE, Seppala K, Kosunen TU *et al.* Eradication of *Helicobacter pylori* improves the healing rate and reduces the relapse rate of nonbleeding ulcers in patients with bleeding peptic ulcer. *Am. J. Gastroenterol.* 2003; **98**: 2149–56.
3. Malfertheiner P, Kirchner T, Kist M *et al. Helicobacter pylori* eradication and gastric ulcer healing–comparison of three pantoprazole-based triple therapies. *Aliment. Pharmacol. Ther.* 2003; **17**: 1125–35.
4. Marshall BJ, Warren JR. Unidentified curved bacilli in the stomach of patients with gastritis and peptic ulceration. *Lancet* 1984; **1**: 1311–15.
5. Malfertheiner P, Chan FK, McColl KE. Peptic ulcer disease. *Lancet* 2009; **374**: 1449–61.
6. Ramakrishnan K, Salinas RC. Peptic ulcer disease. *Am. Fam. Physician.* 2007; **76**: 1005–12.
7. Leung WK, Wu MS, Kakugawa Y *et al.* Screening for gastric cancer in Asia: Current evidence and practice. *Lancet Oncol.* 2008; **9**: 279–87.
8. Yoshida S, Kozu T, Gotoda T *et al.* Detection and treatment of early cancer in high-risk populations. *Best Pract. Res. Clin. Gastroenterol.* 2006; **20**: 745–65.
9. Uedo N, Takeuchi Y, Yamada T *et al.* Effect of a proton pump inhibitor or an H2-receptor antagonist on prevention of bleeding from ulcer after endoscopic submucosal dissection of early gastric cancer: A prospective randomized controlled trial. *Am. J. Gastroenterol.* 2007; **102**: 1610–16.
10. Takizawa K, Oda I, Gotoda T *et al.* Routine coagulation of visible vessels may prevent delayed bleeding after endoscopic submucosal dissection–an analysis of risk factors. *Endoscopy* 2008; **40**: 179–83.
11. Kakushima N, Yahagi N, Fujishiro M *et al.* The healing process of gastric artificial ulcers after endoscopic submucosal dissection. *Dig. Endosc.* 2004; **16**: 327–31.
12. Kakushima N, Fujishiro M, Yahagi N *et al. Helicobacter pylori* status and the extent of gastric atrophy do not affect ulcer healing after endoscopic submucosal dissection. *J. Gastroenterol. Hepatol.* 2006; **21**: 1586–9.
13. Lee SY, Kim JJ, Lee JH *et al.* Healing rate of EMR-induced ulcer in relation to the duration of treatment with omeprazole. *Gastrointest. Endosc.* 2004; **60**: 213–7.
14. Oda I, Gotoda T, Hamanaka H *et al.* Endoscopic submucosal dissection for early gastric cancer: Technical feasibility, operation time and complications from a large consecutive series. *Dig. Endosc.* 2005; **17**: 54–8.
15. Okano A, Hajiro K, Takakuwa H *et al.* Predictors of bleeding after endoscopic mucosal resection of gastric tumors. *Gastrointest. Endosc.* 2003; **57**: 687–90.
16. Goto O, Fujishiro M, Kodashima S *et al.* A second-look endoscopy after endoscopic submucosal dissection for

gastric epithelial neoplasm may be unnecessary: A retrospective analysis of postendoscopic submucosal dissection bleeding. *Gastrointest. Endosc.* 2010; **71**: 241–8.
17. Gotoda T, Yanagisawa A, Sasako M *et al.* Incidence of lymph node metastasis from early gastric cancer: Estimation with a large number of cases at two large centers. *Gastric. Cancer* 2000; **3**: 219–25.
18. Huang JQ, Sridhar S, Hunt RH. Role of *Helicobacter pylori* infection and non-steroidal anti-inflammatory drugs in peptic-ulcer disease: A meta-analysis. *Lancet* 2002; **359**: 14–22.
19. Sakamoto C, Sugano K, Ota S *et al.* Case-control study on the association of upper gastrointestinal bleeding and non-steroidal anti-inflammatory drugs in Japan. *Eur. J. Clin. Pharmacol.* 2006; **62**: 765–72.
20. Messer J, Reitman D, Sacks HS *et al.* Chalmers TC. Association of adrenocorticosteroid therapy and peptic-ulcer disease. *N. Engl. J. Med.* 1983; **309**: 21–4.
21. Kakushima N, Fujishiro M, Kodashima S *et al.* Learning curve for endoscopic submucosal dissection of gastric epithelial neoplasms. *Endoscopy* 2006; **38**: 991–5.
22. Ono H, Kondo H, Gotoda T *et al.* Endoscopic mucosal resection for treatment of early gastric cancer. *Gut* 2001; **48**: 225–9.
23. Fujishiro M, Kodashima S, Goto O *et al.* Technical feasibility of endoscopic submucosal dissection of gastrointestinal epithelial neoplasms with a splash-needle. *Surg. Laparosc. Endosc. Percutan. Tech.* 2008; **18**: 592–7.
24. Yamamoto H, Kawata H, Sunada K *et al.* Success rate of curative endoscopic mucosal resection with circumferential mucosal incision assisted by submucosal injection of sodium hyaluronate. *Gastrointest. Endosc.* 2002; **56**: 507–12.
25. Sakita T, Fukutomi H. Endoscopic diagnosis. In: Yoshitoshi Y (ed.). *Ulcer of the Stomach and Duodenum.* Tokyo: Nankodo, 1971; 198–208. (in Japanese)
26. Vakil N, Fennerty MB. Direct comparative trials of the efficacy of proton pump inhibitors in the management of gastro-oesophageal reflux disease and peptic ulcer disease. *Aliment. Pharmacol. Ther.* 2003; **18**: 559–68.
27. Kakushima N, Fujishiro M, Kodashima S *et al.* Histopathologic characteristics of gastric ulcers created by endoscopic submucosal dissection. *Endoscopy* 2006; **38**: 412–5.
28. Hashimoto T, Adachi K. Changes in gastric mucosal blood flow during healing of EMR-induced ulcer-comparison with peptic ulcer. *Dig. Endosc.* 1997; **9**: 127–31.
29. Tarnawski A, Stachura J, Durbin T *et al.* Increased expression of epidermal growth factor receptor during gastric ulcer healing in rats. *Gastroenterology* 1992; **102**: 695–8.
30. Shay H, Sunn DCH. Etiology and pathology of gastric and duodenal ulcer. In: Bockus HL (ed.). *Gastroenterology*, 2nd edn. Philadelphia & London: WB Saunders, 1996; 420–65.
31. Mannen K, Tsunada S, Hara M *et al.* Risk factors for complications of endoscopic submucosal dissection in gastric tumors: Analysis of 478 lesions. *J. Gastroenterol.* 2010; **45**: 30–6.
32. Oi M, Ito Y, Kumagai F *et al.* A possible dual control mechanism in the origin of peptic ulcer. A study on ulcer location as affected by mucosa and musculature. *Gastroenterology* 1969; **57**: 280–93.
33. Fukase K, Kato M, Kikuchi S *et al.* Effect of eradication of *Helicobacter pylori* on incidence of metachronous gastric carcinoma after endoscopic resection of early gastric cancer: An open-label, randomised controlled trial. *Lancet* 2008; **372**: 392–7.
34. Ono S, Fujishiro M, Niimi K *et al.* Technical feasibility of endoscopic submucosal dissection for early gastric cancer in patients taking anti-coagulants or anti-platelet agents. *Dig. Liver Dis.* 2009; **41**: 725–8.

Biochemical and Biophysical Research Communications 424 (2012) 124–129

Contents lists available at SciVerse ScienceDirect

Biochemical and Biophysical Research Communications

journal homepage: www.elsevier.com/locate/ybbrc

Rebamipide induces dendritic cell recruitment to *N*-methyl-*N'*-nitro-*N*-nitrosoguanidine (MNNG)-exposed rat gastric mucosa based on *IL-1β* upregulation

Nobutake Yamamichi [a,*], Masashi Oka [b,2], Ken-ichi Inada [c,3], Maki Konno-Shimizu [a,1], Natsuko Kageyama-Yahara [a,1], Hideyuki Tamai [b,2], Jun Kato [b,2], Mitsuhiro Fujishiro [a,1], Shinya Kodashima [a,1], Keiko Niimi [a,1], Satoshi Ono [a,1], Yutaka Tsutsumi [c,3], Masao Ichinose [b,2], Kazuhiko Koike [a,1]

[a] *Department of Gastroenterology, Graduate School of Medicine, The University of Tokyo, 7-3-1 Hongo, Bunkyo-ku, Tokyo 113-8655, Japan*
[b] *Department of Gastroenterology, School of Medicine, Wakayama Medical University, 811-1 Kimiidera, Wakayama-shi, Wakayama 641-0012, Japan*
[c] *1st Department of Pathology, Fujita Health University School of Medicine, 1-98 Dengakugakubo, Kutsukake-cho, Toyoake, Aichi 470-1192, Japan*

ARTICLE INFO

Article history:
Received 5 June 2012
Available online 23 June 2012

Keywords:
Rebamipide
Gastric cancer
N-methyl-*N'*-nitro-*N*-nitrosoguanidine
Dendritic cell
IL-1β
CD68

ABSTRACT

Rebamipide is usually used for mucosal protection, healing of gastric ulcers, treatment of gastritis, etc., but its effects on gastric malignancy have not been elucidated. Using Lewis and Buffalo rat strains treated with peroral administration of *N*-methyl-*N'*-nitro-*N*-nitrosoguanidine (MNNG), we evaluated the effect of rebamipide on the induction of tumor-suppressive dendritic cells, which are known to be heterogeneous antigen-presenting cells of bone marrow origin and are critical for the initiation of primary T-cell responses. Using CD68 as a marker for dendritic cells, the stomach pyloric mucosae of Lewis and Buffalo rats were immunohistochemically analyzed in the presence or absence of rebamipide and MNNG. After a 14-day treatment of rebamipide alone, no significant change in number of CD68-expressing cells was detected in either rat strain. However, after concurrent exposure to MNNG for 14 days, treatment with rebamipide slightly increased CD68-positive cells in the Lewis strain, and significantly increased them in the Buffalo strain. Analysis of two chemotactic factors of dendritic cells, IL-1β and TNF-α, in the gastric cancer cells showed that expression of *IL-1β*, but not *TNF-α*, was induced by rebamipide in a dose-dependent manner. A luciferase promoter assay using gastric SH-10-TC cells demonstrated that an element mediating rebamipide action exists in the *IL-1β* gene promoter region. In conclusion, rebamipide has potential tumor-suppressive effects on gastric tumorigenesis via the recruitment of dendritic cells, based on the upregulation of the *IL-1β* gene in gastric epithelial cells.

1. Introduction

Rebamipide, an amino acid analog of 2(1H)-quinolinone, is clinically used for mucosal protection, healing of gastric ulcers, and treatment of gastritis [1,2]. The healing effects depend on the enhancement of mucosal defense, scavenging free radicals, and activation of genes such as cyclooxygenase-2 and some growth factors [2]. In the view of carcinogenesis, however, reports concerning the effects of rebamipide on gastric malignancy have been scarce. In this study, we focused on the recruitment of dendritic cells to examine whether rebamipide has a tumor-suppressive effect on gastric mucosa.

Dendritic cells are heterogeneous antigen-presenting cells of bone marrow origin that are critical for the initiation of primary T-cell responses [3,4]. They are thought to play key roles in tumor-specific immune responses via (1) cross-priming of tumor cells and dendritic cells, (2) presentation of tumor antigens through MHC class I, and (3) the generation of CD8+ cytolytic T-cells [4]. We have previously demonstrated that dendritic cells infiltrate the mesenchymal layer of rat stomach during chemical carcinogenesis induced by administration of *N*-methyl-*N'*-nitro-*N*-nitrosoguanidine (MNNG) [5]. In our previous study using ACI (sensitive to chemically induced carcinogenesis) and Buffalo (resistant to chemically induced carcinogenesis) rat strains, we observed

Abbreviations: MNNG, *N*-methyl-*N'*-nitro-*N*-nitrosoguanidine; IL-1β, interleukin-1β; TNF-α, tumor necrosis factor-α.

* Corresponding author. Fax: +81 358 00 8806.
E-mail address: nyamamic-tky@umin.ac.jp (N. Yamamichi).
[1] Fax: +81 358 00 8806.
[2] Fax: +81 734 45 3616.
[3] Fax: +81 562 93 3063.

0006-291X/$ - see front matter © 2012 Elsevier Inc. All rights reserved.
http://dx.doi.org/10.1016/j.bbrc.2012.06.087

a negative correlation between the susceptibility to MNNG-induced carcinogenesis and induction of dendritic cells [5,6].

In the present study, we examined the effect of rebamipide on the recruitment of dendritic cells to the gastric mucosa, using CD68 as a dendritic cell marker [7,8]. In addition, focusing on the candidate chemotactic factors of dendritic cells, we examined the effect of rebamipide on gastric cells by analyzing the gene expression of two cytokines, IL-1β and TNF-α, involved in dendritic cell mobilization. Our study should shed light on a novel effect of rebamipide on the precancerous gastric mucosa.

2. Materials and methods

2.1. Animals

Forty male 6-week-old Lewis rats (LEW/Crj; Charles River Japan, Inc., Yokohama, Japan) and 40 male 6-week-old Buffalo rats (BUF/NacJCl; Nihon Clea, Tokyo, Japan) were used. Based upon the combination of drinking water and food (CRF1, Oriental. Yeast Co., Ltd., Tokyo, Japan) provided, the rats were divided into four groups, with 10 rats in each group, as follows: (1) water with 120 mg/l of MNNG (Sigma–Aldrich, St. Louis, MO) and food with 0.25% w/w rebamipide (Sigma–Aldrich), (2) water with 120 mg/l of MNNG and normal food, (3) normal water and food with 0.25% w/w rebamipide, and (4) normal water and normal food. Treatment of animals used in this study adhered to the Declaration of Helsinki.

2.2. Immunohistochemistry

Deparaffinization, endogenous peroxidase inactivation, and antigen retrieval of rat stomach tissues were performed as described previously [9,10]. Immunostaining with anti-CD68 mouse monoclonal antibody (Clone: KP1; DAKO, Tokyo, Japan) at a 1:200 dilution was performed, followed by visualization with 20 mg/dl 3,3′-diaminobenzidine tetrahydrochloride (DAKO) solution containing 0.006% hydrogen peroxide. The immunostained sections were evaluated independently by two pathologists along with hematoxylin and eosin-stained sections from the same lesions.

2.3. Cell cultures

Twenty gastric cancer cell lines (NUGC-4, AZ521, KATO-III, SH-10-TC, MKN-7, H-III-TC, MKN-1, MKN-45, MKN-74, TGBC11TKB, KE-39, KE-97, GCIY, HGC-27, HuG1-PI, HuG1-N, AGS, NCI-N87, ECC-10, ECC-12), 10 colorectal cancer cell lines (WiDr, DLD-1, SW480, COLO320DM, HCT116, HCT-15, SW620, LS174T, LOVO, HT-29), and two non-gastrointestinal cancer cell lines (HeLa-S3 and MDA-MB435) were maintained in DMEM with 10% fetal calf serum (Gibco/Invitrogen, Carlsbad, CA) at 37 °C, as previously reported [11]. Rebamipide at concentrations of 6, 2, 0.7, and 0 mM in culture medium (DMEM with 10% fetal calf serum) was used for treatment.

2.4. RT-PCR

Total cellular RNAs were prepared using the Isogen RNA isolation reagent (Wako Pure Chemical Industries, Osaka, Japan) as previously reported [12]. Semi-quantitative RT-PCR was performed via a Superscript One-Step reaction using the Platinum Taq (Invitrogen). The primer pairs used to detect the transcripts of *TNF-α*, *IL-1β*, and *GAPDH* were as follows: 5′-gtgcttgttcctcagcctct-3′ and 5′-ttgatggcagagaggaggtt-3′ for *TNF-α*, 5′-tccagggacaggatatggag-3′ and 5′-ccctagggattgagtccaca-3′ for *IL-1β*, and 5′-accacagtccatgccatcac-3′ and 5′-tccaccaccctgttgctgta-3′ for *GAPDH*. RNA was reverse-transcribed for 30 min at 50 °C, and after an initial denaturation at 94 °C for 3 min, cDNA amplification procedures were performed as follows: for *TNF-α* and *IL-1β*, 40 cycles of 94 °C for 30 s, 58 °C for 1 min, and 72 °C for 1 min; for *GAPDH*, 24 cycles of 94 °C for 30 s, 58 °C for 1 min, and 72 °C for 1 min.

2.5. Luciferase promoter assay

SH-10-TC cells were seeded in 96-well (0.32 cm^2) plates in a semi-confluent manner in the presence or absence of 6 mM rebamipide in medium for 24 h. They were then transfected with 6.5 ng of Renilla luciferase control vector pGL4.74 (Promega, Madison, WI), and either 200 ng of firefly luciferase experimental vector pGL4.12 (Promega, negative control), pGL4.12_IL-1β-P1 (upstream 1062 bp from the exon 1 of *IL-1β*), pGL4.12_IL-1β-P2 (upstream 513 bp), pGL4.12_IL-1β-P3 (upstream 131 bp), or pGL4.12-TK (positive control). All transfections were performed with Lipofectamine Reagent and Lipofectamine PLUS (Invitrogen). Luciferase activities were measured at 48 h post-transfection using the Dual Luciferase Reporter Assay System (Promega).

2.6. Constructions

To construct the vectors for reporter assays, a 1500-bp upstream sequence from the 5′-end of exon 1 of the *IL-1β* gene was first amplified from genomic DNA derived from SH-10-TC cells using the primers 5′-atacttgcacagaggctcac-3′ and 5′-gattggctgaagagaatccc-3′. The amplified products were cloned into pT7blue T-vector cloning vectors (TAKARA Bio Inc., Shiga, Japan) to generate pT7Blue-IL-1β-P0. The 1.6-kb DNA BamHI/SpeI fragment was blunted with Klenow fragment (TAKARA) and inserted into the EcoRV site of pGL4.12 (Promega) to generate pGL4.12-IL-1β-P0. After the 5.5-kb XhoI/SmaI fragment derived from pGL4.12-IL-1β-P0 was blunted with Klenow fragment, self-ligation was performed to generate pGL4.12-IL-1β-P1 (upstream 1062 bp). The 5.0-kb SacI fragment derived from pGL4.12-IL-1β-P0 was also self-ligated to generate pGL4.12-IL-1β-P2 (upstream 513 bp). The 0.15-kbp HindIII/BamHI fragment derived from pT7Blue-IL-1β-P0 was inserted into EcoRV site of pGL4.12 to generate pGL4.12-IL-1β-P3 (upstream 131 bp). For positive control, the 0.8 kb HindIII/KpnI fragment (human simplex virus thymidine kinase gene promoter) derived from pGL4.74 (Promega) was inserted into HindIII/KpnI site of pGL4.12 to generate pGL4.12-TK.

3. Results

3.1. Treatment with rebamipide increases the number of dendritic cells in MNNG-exposed rat gastric mucosa

To evaluate the effect of rebamipide on the gastric mucosa, we analyzed the expression of CD68-positive cells in the stomach pyloric mucosa of Lewis and Buffalo rat strains. CD68 is an established marker of dendritic cells, and CD68-positive cells in the gastric mucosa can be considered as dendritic cells [7,8,13]. After the 14-day treatment of rebamipide alone, an obvious microscopic change of the gastric mucosa could not be detected in both Lewis and Buffalo strains. There were also no significant differences in the number of CD68-positive cells with or without the 14-day treatment of rebamipide (Fig. 1A and 1B).

We next analyzed the effect of rebamipide on the recruitment of CD68-positive cells in the stomach pyloric mucosa of the MNNG-exposed Lewis and Buffalo rats. Consistent with previous reports [14,15], neither intestinal metaplasia nor adenocarcinoma could be observed in the gastric mucosa after the treatment of MNNG for only 14 days. We have already reported that the number of dendritic cells in the rat stomach pyloric mucosa increase after

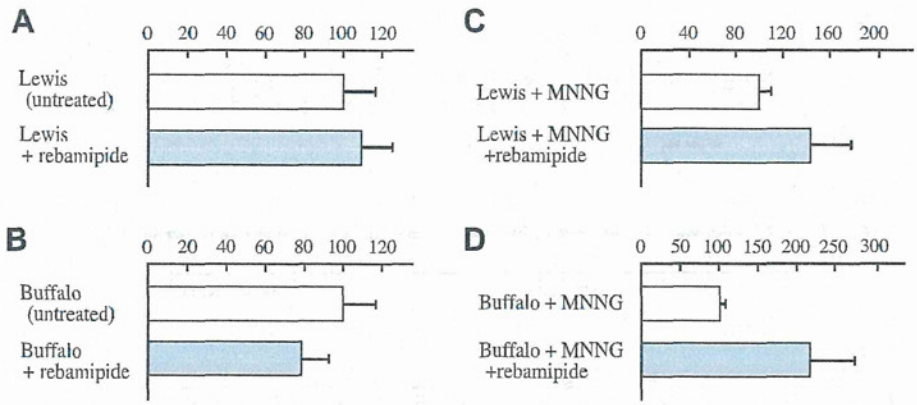

Fig. 1. Numbers of CD68-positive cells in the gastric pyloric mucosa of Lewis and Buffalo rat strains in a single microscopic view (200×). Data were obtained from the eight groups of 10 rats as follows: (A) Lewis untreated (control) and Lewis treated with rebamipide for 14 days; (B) Buffalo untreated (control) and Buffalo treated with rebamipide for 14 days; (C) Lewis treated with MNNG alone for 14 days and Lewis treated with a combination of MNNG and rebamipide for 14 days; and (D) Buffalo treated with MNNG alone for 14 days and Buffalo treated with a combination of MNNG and rebamipide for 14 days. In each panel, the number of CD68-positive cells was standardized to that of the rats without rebamipide treatment. About 120 mg/l of MNNG in drinking water and 0.25% w/w of rebamipide in food were used as treatments. The error bars indicate the standard errors based on the data obtained from corresponding 10 rats.

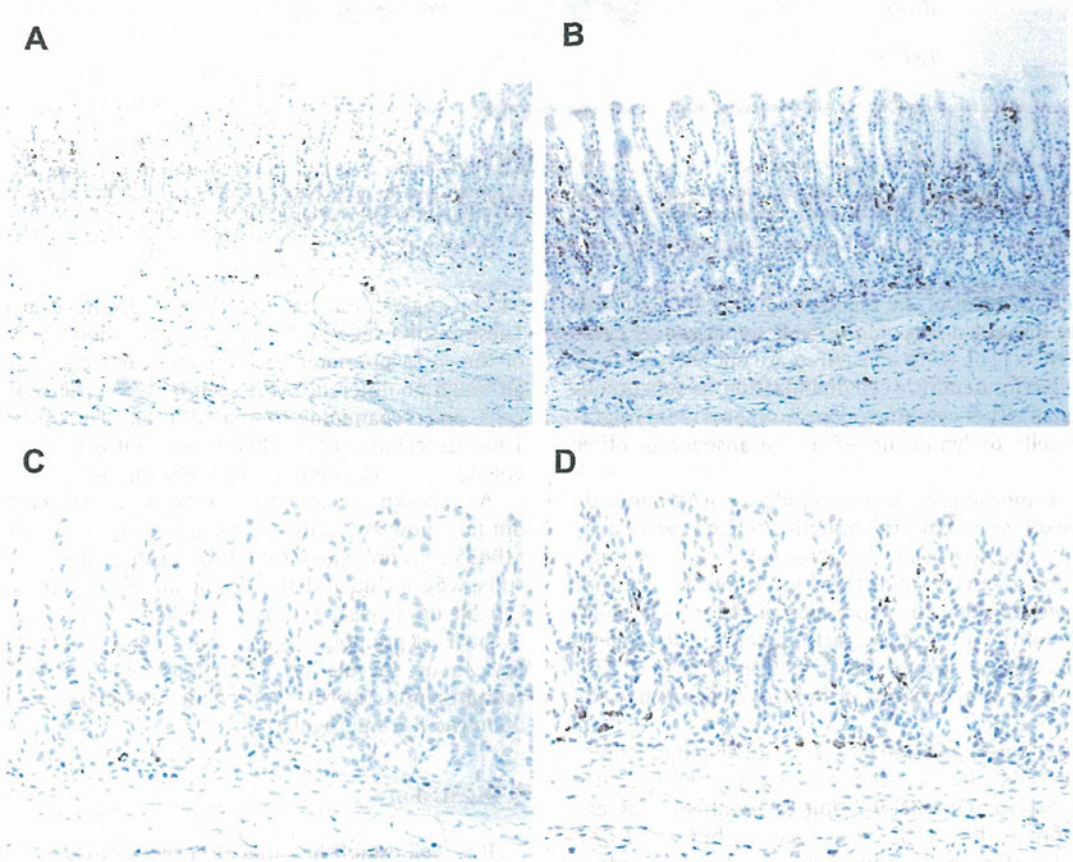

Fig. 2. Immunohistochemical staining of CD68 in gastric pyloric tissue sections obtained from Lewis and Buffalo rats. Magnification 200×. (A) Lewis strain rats treated with MNNG alone for 14 days. (B) Lewis strain rats treated with a combination of MNNG and rebamipide for 14 days. (C) Buffalo strain rats treated with MNNG alone for 14 days. (D) Buffalo strain rats treated with a combination of MNNG and rebamipide for 14 days. About 120 mg/l of MNNG in drinking water and 0.25% w/w of rebamipide in food were used as treatments.

exposure to MNNG [5]. In the Lewis strain, induction of CD68-positive cells seemed to be stronger with rebamipide treatment (Fig. 2A and 2B), although statistical significance could not be obtained (Fig. 1C). As for the Buffalo strain, a significant increase in CD68-positive dendritic cells was detected with the rebamipide treatment (Figs. 2C, 2D and 1D). From these results, we concluded that oral rebamipide intake has the potential to induce the migration of dendritic cells to the gastric mucosa. Rebamipide and MNNG possibly have an addictive or multiplier effect on the dendritic cell migration.

3.2. Treatment with rebamipide activates the transcription of IL-1β, a potent chemotactic factor for dendritic cells, in various gastric cell lines

It is well established that dendritic cells are mobilized in response to a large variety of chemical, physical, or biological stimuli.

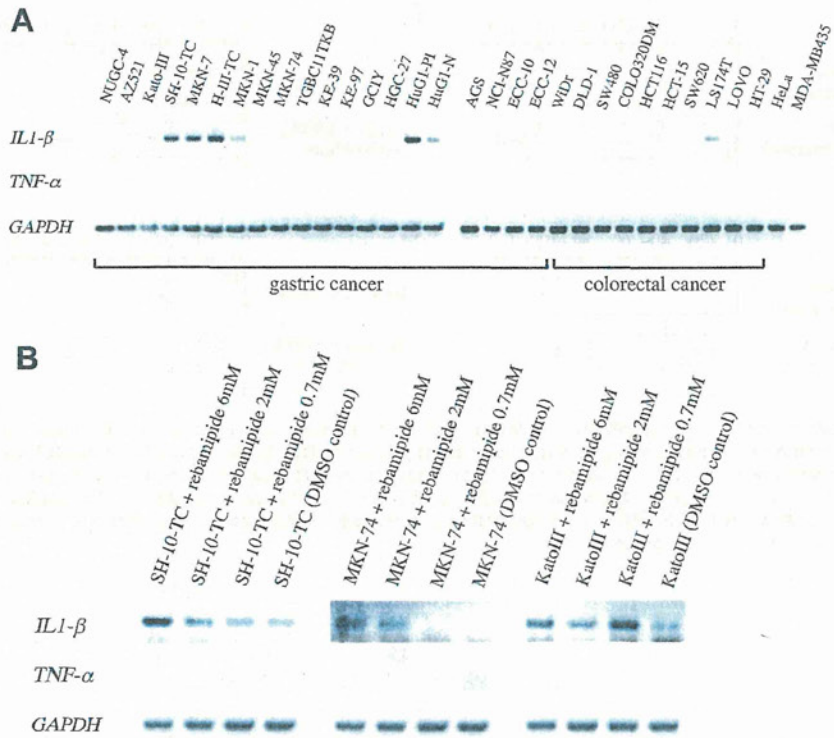

Fig. 3. (A) Expression patterns of *IL-1β*, *TNF-α*, and *GAPDH* mRNAs in a panel of 32 human cancer cell lines. Twenty gastric cancer cell lines, 10 colorectal cell lines, and two non-gastrointestinal cell lines (HeLa-S3 and MDA-MB435) were analyzed by RT-PCR. (B) Expression of *IL-1β*, *TNF-α*, and *GAPDH* after a 2-day treatment of rebamipide at various concentration (6, 2, 0.7, or 0 mM). Three gastric cancer cell lines (SH-10-TC, MKN-74, and KATO-III) were analyzed by RT-PCR.

Despite their diversity, most of the mobilization signals appear to exert their activity through a pair of intermediate messenger cytokines, IL-1β and TNF-α [16]. IL-1β and TNF-α are not only required but are also sufficient for dendritic cell mobilization, as subcutaneous administration of either cytokines alone promotes rapid migration of dendritic cells to lymph nodes in the absence of other stimuli [17,18].

To elucidate the mechanism of rebamipide-induced dendritic cell recruitment, expression patterns of both cytokines were analyzed using twenty gastric cell lines and 10 colorectal cell lines. *TNF-α* mRNA was barely detected in these gastrointestinal tumor cells (Fig. 3A), suggesting that the expression of TNF-α is strongly suppressed in cells of the alimentary tract. In contrast, *IL-1β* gene transcript was detected in several gastric cancer cells (Fig. 3A); we speculate that IL-1β may be a major inducer of dendritic cells during gastric canceration.

Next, we analyzed the expression of *IL-1β* and *TNF-α* in the presence of rebamipide at various concentrations using three gastric cancer cell lines: SH-10-TC, MKN-74, and KATO-III. As was expected, marked upregulation of *IL-1β* expression, but not *TNF-α* expression, was detected in an approximately dose-dependent manner (Fig. 3B). From these results, we concluded that rebamipide treatment activates transcription of *IL-1β* in gastrointestinal cells.

3.3. The element mediating rebamipide action in gastric cells exists in the promoter region of IL-1β gene

To elucidate the mechanism of rebamipide-induced *IL-1β* upregulation, we designed a series of reporter constructs using the upstream sequence of *IL-1β* gene and performed a luciferase assay in SH-10-TC cells (Fig. 4). The upstream 131 bp (P3) alone did not express the reporter luciferase gene, whereas the upstream 513 bp region (P2) had an obvious promoter activity (Fig. 4B). These results suggest that the sequence between −513 and −131 of the *IL-1β* promoter has promoter activity in the gastric cells, although no difference was seen between the rebamipide-treated cells and rebamipide-untreated cells (Fig. 4B). The upstream 1062 bp region (P1) also had an evident promoter activity, which got stronger in the presence of rebamipide.

As was expected, the three reporter constructs (P1, P2, and P3) did not show any transcriptional activity in IL-1β-deficient MDA-MB435 cells originated from breast cancer (Fig. 4B). From these results, we concluded that an element mediating rebamipide action, capable of increasing transcriptional activity in gastric cells, exists in the *IL-1β* promoter region from −1062 to −513. This result reinforces our speculation that rebamipide-induced dendritic cell recruitment to MNNG-exposed rat gastric mucosa should be based upon the *IL-1β* upregulation.

4. Discussion

It is well established that *Helicobacter pylori*-associated chronic gastritis is a precancerous condition of gastric malignancy [19,20]. Although the effects of rebamipide on gastric malignancy have been barely elucidated, there have been some reports concerning its tumor-suppressive effects via an influence on gastritis or gastric cancer cells. For instance, it was reported that rebamipide inhibits the production of neutrophil chemokines (CINC/KC) and TNF-α, and consequently prevents the development of chronic gastritis [21]. In the gastric cancer mouse model induced by *N*-methyl-*N*-nitrosourea (NMU) treatment and *Helicobacter pylori* infection, it was also reported that long-term rebamipide administration inhibits its upregulation of oncogenic proteins and down-regulation of anti-oncogenic proteins in gastric cells [22]. In addition, it was recently reported that rebamipide treatment inhibits gastric cancer